Caenorhabditis elegans SEL-5/AAK1 regulates cell migration and cell outgrowth independently of its kinase activity

Filip Knop[1], Apolena Zounarová[1], Marie Macůrková[1,*]

[1] Department of Cell Biology, Faculty of Science, Charles University, Vinicna 7, 128 00 Prague 2, Czech Republic

* Corresponding author

Keywords: SEL-5/AAK1, Wnt signalling, DPY-23/AP2M1, excretory cell, retromer

Abstract

During *Caenorhabditis elegans* development multiple cells migrate long distances or extend processes to reach their final position and/or attain proper shape. Wnt signalling pathway stands out as one of the major coordinators of cell migration or cell outgrowth along the anterior-posterior body axis. Wnt signalling outcome is fine-tuned by various mechanisms including endocytosis. In this study we show that SEL-5, the *C. elegans* orthologue of mammalian AP2-associated kinase AAK1, acts together with the retromer complex as a positive regulator of EGL-20/Wnt signalling during the migration of QL neuroblast daughter cells. At the same time, SEL-5 in cooperation with the retromer complex is also required during excretory canal cell outgrowth in a Wnt-independent manner. Importantly, SEL-5 kinase activity is not required for its role in either neuronal migration or excretory cell outgrowth and neither of these processes is dependent on DPY-23/AP2M1 phosphorylation. While Wnt proteins do not significantly contribute to the excretory canal guidance, LIN-44/Wnt and LIN-17/Frizzled together generate a stop signal inhibiting further canal outgrowth.

Introduction

During the development of *Caenorhabditis elegans* several cells, both neuronal and non-neuronal, migrate in a well-defined and invariant manner along the anterior-posterior (A-P) body axis. Other cells do not migrate but rather extend their processes along the same axis. In both instances the directionality of migration and growth is controlled by a set of guidance cues provided by the surrounding tissue and received by the corresponding signalling apparatus in the migrating or growing cell (Silhankova and Korswagen, 2007; Sundaram and Buechner, 2016; Sherwood and Plastino, 2018; Hutter, 2019). Gradients of Wnt proteins and panel of their receptors are the key determinants of the A-P guidance in *C.elegans*. Wnts can

act either as attractants, repellents or as permissive cues for given cell and the cell response depends on a given combination of Wnts, Frizzleds and other components of the Wnt pathway expressed in and around that particular cell (Silhankova and Korswagen, 2007; Ackley, 2014; Middelkoop and Korswagen, 2014; Rella et al., 2016).

Endocytosis is an important regulatory mechanism of Wnt signalling applied in both Wnt producing and Wnt receiving cells. On the way out of the producing cell Wnts are accompanied by a Wnt sorting receptor Wntless (WLS) (Banziger et al., 2006; Bartscherer et al., 2006; Goodman et al., 2006). Once WLS is relieved of its cargo at the plasma membrane, it is internalized by clathrin- and adaptor protein complex 2 (AP2)-dependent endocytosis (Pan et al., 2008; Port et al., 2008; Yang et al., 2008). Internalized WLS is subsequently recycled by a multisubunit retromer complex to the Golgi apparatus (Belenkaya et al., 2008; Franch-Marro et al., 2008; Pan et al., 2008; Port et al., 2008; Yang et al., 2008) and further to the endoplasmic reticulum (Yu et al., 2014). Disruption of AP2 or clathrin function results in decreased Wnt secretion due to improper WLS recycling (Pan et al., 2008; Port et al., 2008; Yang et al., 2008). In Wnt receiving cells, the activity of the Wnt-receptor complex, the signalosome, can be promoted by endocytosis, while at the same time endocytosis can also attenuate Wnt signalling by regulating the membrane availability of Wnt receptors (Albrecht et al., 2021; Colozza and Koo, 2021; Wu et al., 2021).

AP2-associated kinase 1 (AAK1) belongs to the Ark/Prk or Numb-associated (NAK) family of serine/threonine protein kinases (Smythe and Ayskough, 2003; Sorrell et al., 2016). Members of this family play an important role in regulating endocytosis in yeast, *Drosophila* or mammals (Smythe and Ayskough, 2003; Peng et al., 2009). Human AAK1 has been shown to phosphorylate AP2M1, the μ2 subunit of the AP2 adaptor complex (Conner and Schmid, 2002). Phosphorylation of μ2 at Thr156 by AAK1 enhances the binding affinity of AP2 to sorting signals of endocytosed proteins (Ricotta et al., 2002). AAK1 has also been shown to

phosphorylate the endocytic adaptor and negative regulator of Notch signalling Numb and affect its subcellular localization (Sorensen and Conner, 2008). Interestingly, AAK1 can also interact with membrane-tethered activated form of Notch receptor and promote its internalization (Gupta-Rossi et al., 2011).

AAK1 knock-down upregulated Wnt signalling in a mouse embryonic stem cell-based kinase and phosphatase siRNA screen (Groenendyk and Michalak, 2011). Recent study in human cells confirmed this observation and offered a mechanism. By phosphorylating AP2 AAK1 promotes endocytosis of LRP6 and thus shuts down the signalling (Agajanian et al., 2018). In *C. elegans*, AAK1 orthologue SEL-5 has been genetically implicated in Notch signalling as mutation in *sel-5* can suppress the constitutively active *lin-12*/Notch mutants. Suppression is however observed only in *lin-12* allele activating the membrane-anchored Notch and not when the pathway is activated by expression of the intracellular domain (Fares and Greenwald, 1999). This hints that SEL-5 could regulate endocytosis in a similar manner as its mammalian counterpart. So far, no link has been made between SEL-5 and *C. elegans* Wnt signalling regulation.

In this study we set to analyse the potential role of the SEL-5 kinase in Wnt signalling regulation and its contribution to DPY-23/AP2M1 phosphorylation in *C. elegans*. We show that SEL-5 acts in collaboration with the retromer complex as a positive regulator of EGL-20/Wnt signalling during the migration of QL neuroblast descendants. We further demonstrate that although SEL-5 participates on DPY-23 phosphorylation, the observed role of SEL-5 in neuroblast migration is independent of its kinase activity and the phosphorylation of DPY-23 is dispensable for Wnt-dependent migration of QL neuroblast descendants. SEL-5 together with the retromer is further required during the active phase of excretory cell canal extension, again independently of its kinase activity. Finally we show that Wnt proteins do

not serve as major guidance cues for excretory canal outgrowth but LIN-44/Wnt and LIN-17/Frizzled together define the stopping point for canal extension.

Results

Loss of SEL-5 affects migration of QL neuroblast descendants

Q cell descendant (Q.d) migration is dependent on EGL-20/Wnt signalling. While on the right side of the L1 larva QR divides and QR.d migrate in the default anterior direction, on the left side QL.d respond to the EGL-20 signal produced in several cells around the rectum by expressing homeotic gene *mab-5* and migrate to the posterior. In the absence of active EGL-20 signalling *mab-5* is not expressed and QL.d migrate to the anterior (Salser and Kenyon, 1992) (Fig. 1A). In order to visualize Q.d migration we utilized *Pmec-7::gfp* expressing transgene *muIs32* that is, apart from other cells, active in AVM and PVM touch neurons, which are QR and QL descendants, respectively (Ch'ng et al., 2003). We performed RNA interference (RNAi) against *sel-5* in wild type background and observed no effect on QL.d migration (Fig. 1B). To increase the sensitivity of the RNAi approach, we repeated the RNAi experiment using *vps-29(tm1320)* mutant strain. This strain harbours a null mutation in the VPS-29 retromer subunit, displays only weakly penetrant QL.d migration defect (Coudreuse et al., 2006) and has been used previously as a sensitized background to uncover genes required for the Q.d migration (Harterink et al., 2011; Lorenowicz et al., 2014). RNAi against *sel-5* significantly increased the QL.d migration defect of *vps-29(tm1320)* (Fig. 1B). To verify the results obtained with RNAi we assessed the QL.d migration in *sel-5(ok363)* and *sel-5(ok149)* mutants. Similarly to RNAi results, single *sel-5* mutation had no effect on QL.d migration while *sel-5 vps-29* double mutants displayed almost fully penetrant defect (Fig. 1C, D).

Loss of *vps-29* affects EGL-20/Wnt signalling at the level of Wnt production (Yang et al., 2008). We further tested whether loss of *sel-5* could enhance partially penetrant defects in QL.d migration in mutants acting at different level of the EGL-20/Wnt pathway. Loss of *sel-5* strongly increased the weak QL.d migration defect of the *lin-17*/Frizzled mutants but had no effect on the already more penetrant QL.d defect of *mig-1*/Frizzled mutant animals (Fig. 1D).

We next asked whether loss of *sel-5* in the *vps-29* background affects other Wnt-dependent processes such as the polarization of the ALM and PLM neurons, CAN neuron migration or T cell polarity. Polarization of ALM and PLM is regulated by several Wnt proteins (Pan et al., 2006; Prasad and Clark, 2006; Hilliard and Bargmann, 2006), CAN neuron migration is governed predominantly by CWN-2 with minor contribution from CWN-1 and EGL-20 (Zinovyeva and Forrester, 2005; Zinovyeva et al., 2008) and T cell polarity depends on the LIN-44/Wnt signal (Herman et al., 1995). We observed weakly penetrant ALM polarization defects in both *sel-5(ok363) vps-29* and *sel-5(ok149) vps-29* double mutants, a very mild PLM polarization defect was detected in a strain carrying the *ok149* allele (Table 1). Mildly penetrant anterior displacement of the CAN neuron was observed in the double mutants, while about 17% of double mutant animals carrying the *ok149* allele did not correctly form the phasmid sensillum which indicates defects in T cell polarization (Table 1). Apart from these Wnt dependent phenotypes, we also observed reduced brood size in the double mutants compared to controls (Table 1) and defective tail formation (Fig. 1E).

The penetrance of the observed phenotypes was not the same in the two *sel-5* alleles. This was striking as both alleles carry deletions hitting the kinase domain of SEL-5 protein. We were able to amplify shorter than wild type transcripts from both *sel-5(ok363)* and *sel-5(ok149)* animals using primers in exon 1 and exon 17 (Fig. 1F). Sequencing of the *ok363* transcript revealed that amino acids 1 to 243 of the wild type protein followed by extra 32 amino acids would be translated due to a frameshift and a premature stop codon. Such protein

encompasses larger part of the SEL-5 kinase domain including the active site. In agreement with data published by Fares and Greenwald (Fares and Greenwald, 1999), sequencing of *ok149* transcript revealed that it can give rise to a protein containing the first 153 amino acids of SEL-5 followed by 21 extra amino acids and is thus devoid of the active site (Fig. 1F). If such truncated proteins are present in the mutants, it is possible that either one or both possess some residual activity that is responsible for the observed phenotypic differences.

SEL-5 is required in EGL-20/Wnt producing cells to direct QL.d migration

The asymmetric migration of the Q neuroblast is regulated both cell-autonomously and non-autonomously. To analyse the tissue-specific requirement of SEL-5 in QL.d migration we expressed full-length SEL-5 tagged with GFP at its N-terminus under the control of different tissue-specific promoters in *sel-5 vps-29* background and assayed the QL.d migration. Expression of SEL-5 from *egl-20* promoter (Coudreuse et al., 2006) resulted in a significant rescue of the QL.d migration defect of *sel-5 vps-29* double mutants albeit not to the level of *vps-29* single mutant (Fig. 2A). No rescue was obtained when SEL-5 was expressed from the *wrt-2* promoter that is active in the seam cells and in the Q cell (Aspock et al., 1999; Middelkoop et al., 2012). These data suggest that *sel-5* is required in the EGL-20/Wnt producing cells to control QL.d migration. However, similar level of rescue as with *egl-20* promoter was obtained also when SEL-5 was expressed from *hlh-1* promoter specific for the body wall muscle cells (Krause et al., 1990, Harfe et al., 1998). When SEL-5 was expressed from *egl-20* and *hlh-1* at the same time, the rescue almost reached the background frequency of the QL.d defect, caused by *vps-29* alone (Fig. 1D, 2A). Apart from the rectal epithelial cells, *egl-20* expression was also detected in posterior ventral body wall muscle quadrants VL23 and VR24 (Harterink et al., 2011), it is thus possible that *hlh-1* promoter-driven expression of SEL-5 in these muscle quadrants is responsible for the observed rescue and only

the combined expression from all EGL-20 producing cells is sufficient to drive a full rescue. Alternatively, the observed rescue pattern could indicate that SEL-5 is required both in the Wnt-producing and in the muscle cells which could for example participate in shaping the Wnt gradient.

To confirm that the tissues identified above in the rescue experiments are tissues with genuine *sel-5* expression we set to determine the endogenous *sel-5* expression pattern which has not been previously analysed. The only published expression data (Fares and Greenwald, 1999) were based on expression from *sel-12* instead of *sel-5* promoter. We generated GFP knock-in strains by inserting GFP into the *sel-5* genomic sequence using the SEC cassette approach (Dickinson et al., 2015). We obtained two strains, one expressing a transcriptional P*sel-5::gfp* reporter and one, after excision of the SEC cassette, an N-terminally tagged GFP::SEL-5 under the control of its own promoter (P*sel-5::gfp::sel-5*). Microscopic analyses of both strains revealed that *sel-5* is expressed broadly, but at low level judged by the GFP signal intensity. The most prominent expression was observed in the gonad from the beginning of its development (Fig. 2B). Expression was further observed in the developing oocytes, in the vulva, in epidermal cells and most notably, in the rectal epithelial cells that are known to produce EGL-20/Wnt (Whangbo and Kenyon, 1999) (Fig. 2B, C). These observations further support our finding that SEL-5 is required in EGL-20/Wnt producing cells to regulate QL.d migration. We could not detect *sel-5* expression in the muscles, although we cannot exclude that low level of expression, below the detection limit using the endogenous locus-tagging approach, is present. Interestingly oocytes and epidermal seam cells expressing the GFP::SEL-5 fusion protein revealed its distinct subcellular localization. Protein localized to punctate structures located close to the cell surface (Fig. 2C). This pattern resembles the subcellular distribution of human AAK1 (Conner and Schmid, 2002) hinting that SEL-5 could be involved in regulating intracellular transport similar to AAK1.

SEL-5-associated phenotypes are independent of DPY-23 phosphorylation

SEL-5 orthologue AAK1 has been implicated in endocytosis regulation (Conner and Schmid, 2002; Ricotta et al., 2002). The obvious candidate that could be affected by SEL-5-dependent endocytosis in Wnt producing cells is the Wnt cargo receptor MIG-14/Wls. Human AAK1 can phosphorylate AP2 subunit μ2 (AP2M1) (Conner and Schmid, 2002; Ricotta et al., 2002) and thus increase AP2 affinity to cargo molecules (Ricotta et al., 2002). It is conceivable that SEL-5 could regulate MIG-14/Wls trafficking at the level of AP2-dependent endocytosis. We first tested whether loss of *sel-5* expression has any effect on the level of phosphorylation of DPY-23 (also known as APM-2), the *C. elegans* μ2 subunit of AP2 complex. A phospho-specific antibody recognizing the phosphorylated threonine T160 (T156 in mammalian AP2M1) of DPY-23 (Hollopeter et al., 2014) revealed a decrease in the level of phosphorylated endogenous DPY-23 in *sel-5* mutants compared to wild type animals (Fig. 3A). Similarly, T160 phosphorylation was reduced on overexpressed GFP-tagged DPY-23 (Fig. 3B). Next we assessed MIG-14 levels and localization in *sel-5 vps-29* mutants. However, as shown in Fig. 3C and D, neither levels nor subcellular distribution of a functional MIG-14::GFP protein changed significantly in *sel-5 vps-29* compared to *vps-29* single mutant. Levels of MIG-14::GFP in *sel-5* single mutants were variable yet on average comparable to wild type. We therefore concluded that the significant increase in QL.d migration defect in *sel-5 vps-29* compared to *vps-29* cannot be attributed to changes in MIG-14/Wls trafficking.

Although it is possible that endocytic cargo other than MIG-14 is affected in *sel-5 vps-29* mutants, we could not exclude the possibility that the observed phenotypes are a consequence of defects in other mechanisms unrelated to DPY-23 phosphorylation. To test this hypothesis we repeated the rescue experiment presented in Fig. 2A now with SEL-5 carrying a point mutation in the kinase active site, D178A. When expressed under the control of *egl-20*

promoter, the mutant SEL-5 protein could still rescue the QL migration phenotype to a similar extent as the wild type version (Fig. 3E). Similar results were obtained when a point mutation was introduced to the ATP binding site, K75A. This indicates that SEL-5 kinase activity is not responsible for the phenotypes observed in *sel-5 vps-29* mutants. We next asked whether the absence of DPY-23 phosphorylation at T160 position leads to defects in QL.d migration. To this end we utilized *dpy-23(mew25)* mutant allele harbouring T160A point mutation (G. Hollopeter and G. Beacham, unpublished). Animals carrying *dpy-23(mew25)* alone or in combination with *sel-5(ok149)* did not show any defects in QL.d migration (Fig. 3F). Variable increase in QL.d migration defects were observed in *vps-29;dpy-23(mew25)* animals, but the penetrance of the defect never reached levels comparable to those in *sel-5 vps-29* mutants (Fig. 1D, 3F). Together these observations strongly suggest that the role of SEL-5 in regulation of QL.d migration is not dependent on its kinase activity and moreover, that DPY-23 phosphorylation at T160 is not a major regulatory event in this process.

The outgrowth of excretory cell canals is impaired in *sel-5 vps-29* mutants

We did not observe any gross morphological defects in the *sel-5 vps-29* double mutant strain. However, in some animals we unexpectedly noticed a severe shortening of the posterior canals of the excretory cell that prompted us to analyse this phenotype in more detail. Excretory cell (also called excretory canal cell) is a large H-shaped cell required for osmoregulation (Buechner et al., 1999; Liegeois et al., 2007). Excretory canal cell body is located near the posterior bulb of the pharynx and four excretory canals emanate from the cell body – two short ones directed to the anterior and two posterior canals extending to the rectum (Fig. 4A). To assess the morphology of the excretory cell we expressed GFP under the control of *pgp-12* promoter which is active exclusively in the excretory cell (Zhao et al., 2004) and analysed the length of the canals in late L4 or early adult animals. While the

posterior canal length in *sel-5* or *vps-29* single mutants was indistinguishable from the wild type controls, in more than 60 % of *sel-5 vps-29* mutants the posterior canals stopped at various positions anterior to the rectum (Fig. 4A,B). Similar effect, albeit with lower penetrance, was observed when assessing the anterior canal length (Fig. 4C). Interestingly, the posterior canal on the right side of the animal was significantly more affected than its counterpart on the left side in *sel-5 vps-29* double mutants carrying the *ok149* allele (Fig. 4D). Similar trend was observed in *sel-5(ok363) vps-29* animals, although the difference observed there did not reach statistical significance (Fig. 4D).

The active growth of the canals starts during embryogenesis and continues during L1, after that the canals passively grow with the growing animal (Fujita et al., 2003). Comparison of canal lengths at several time points within a 24-hour interval after hatching revealed that in *sel-5 vps-29* double mutants the posterior canals of the excretory cell are shorter already at the time of hatching and the growth defect prevails into the larval development (Fig. 4E).

Excretory canal shortening has not previously been reported for any of the retromer components. We therefore tested whether this phenotype is specific for the *vps-29* retromer subunit or whether the whole retromer complex is required together with *sel-5* for proper excretory canal extension. We performed RNAi against *vps-35*, *vps-26*, *snx-1* and *snx-3* in *sel-5(ok149)* background and assessed the posterior canal length. Except for *snx-1* RNAi, significant shortening was observed with RNAi against all other retromer subunits, with *vps-35* showing the strongest phenotype (Fig. 4F). These data confirm that the whole retromer complex acts together with *sel-5* to control excretory canal outgrowth.

We next tested in which tissue SEL-5 activity is required for excretory cell outgrowth. We expressed SEL-5 from either *pgp-12* (excretory cell), *hlh-1* (body wall muscle cells) or *col-10* (hypodermis) promoters in *sel-5 vps-29* double mutants and checked for any rescue. As shown in Fig. 4G, expression of SEL-5 from *pgp-12* promoter almost fully rescued the

excretory cell shortening while SEL-5 expression from the muscle specific *hlh-1* promoter had no effect on the excretory cell phenotype of the *sel-5 vps-29* double mutants. As in the case of QL.d migration defect, the excretory canal length was efficiently rescued also by the SEL-5D178A variant expressed from *pgp-12* promoter arguing that SEL-5 kinase activity is not required for canal extension (Fig. 4G). Expression of VPS-29 in the excretory cell partially rescued the canal shortening suggesting that SEL-5 and the retromer complex act together within the same cell to regulate canal length. Interestingly, expression of SEL-5 from *col-10* promoter which is active in hypodermis (Spencer et al., 2001) also resulted in a significant rescue of the excretory canal shortening. This suggests that SEL-5 activity in both the excretory cell and in the hypodermis contribute to the regulation of the canal outgrowth.

To support our finding that SEL-5 role in excretory canal outgrowth is independent of its kinase activity, we analysed posterior canal length in *dpy-23(mew25)* mutant animals. No canal shortening was observed in animals carrying *dpy-23(mew25)* alone (Fig. 4H), while very mild shortening was occasionally observed in either *sel-5; dpy-23(mew25)* or *vps-29; dpy-23(mew25)*. These observations are consistent with a role of SEL-5 other than DPY-23 phosphorylation at T160.

LIN-44/Wnt-dependent signalling is required to terminate excretory cell canal outgrowth

We were interested whether the observed shortening of the excretory canals in *sel-5 vps-29* mutants could be a consequence of a crosstalk with the Wnt signalling as in the case of QL.d migration. There is some evidence that Wnt pathway components are involved in canal extension regulation. Firstly, *lin-17/Frizzled* mutants have been reported to show an overgrowth of the posterior excretory cell canals past the rectum into the tip of the tail (Hedgecock et al., 1987). Secondly, loss of *axl-1*, one of the two *C. elegans* Axin orthologues,

resulted in ectopic branching of the posterior excretory canal but no effect on the canal length was observed. The ectopic branching in *axl-1* mutants could be rescued by simultaneous loss of *bar-1*/β-catenin or *pop-1*/Tcf expression (Oosterveen et al., 2007). Wnt signalling thus seems to play a role in excretory canal growth, but so far, the other Wnt pathway components and their mechanism of action remained unknown. We therefore decided to test whether mutations in other Wnt pathway components could affect excretory cell growth. Among the four Wnts tested (EGL-20, LIN-44, CWN-1, CWN-2), only mutants in *lin-44*/Wnt exhibited almost fully penetrant posterior excretory canal overgrowth phenotype, as observed in *lin-17*/Frizzled mutants (Fig. 5A, B). Mild canal shortening was observed in *cwn-2*/Wnt and *cfz-2*/Frizzled mutants, while very weak overgrowth phenotype could be detected in *egl-20*/Wnt mutants (Fig. 5B). No change in excretory canal length was displayed by *cwn-1*/Wnt or *mig-1*/Frizzled mutants. Interestingly, highly penetrant canal overgrowth was also observed in *mig-14*/Wls mutants, while loss of *mig-5*/Dishevelled or *dsh-1*/Dishevelled resulted in partially penetrant overgrowth phenotype (Fig. 5B). We next tested various combinations of Wnt and Frizzled mutants and found out that simultaneous loss of *lin-44* and *cwn-1* or *lin-44* and *cwn-2* expression resulted in partial rescue of the canal overgrowth, same effect was observed after simultaneous loss of *lin-17* and *cfz-2*. These data suggest that there are at least two Wnt-dependent pathways acting during the extension of the excretory canal; one involving *lin-44*, *lin-17*, *dsh-1* and *mig-5* that is responsible for determining the stopping point for the growing canal, and one involving *cwn-1*, *cwn-2* and *cfz-2* that contributes to the canal growth.

The most striking phenotype is the overgrowth of the posterior excretory canal in *lin-17*, *lin-44* and *mig-14* mutants. Interestingly when we measured the length of the excretory canal within the 24-hour interval after hatching, no difference in canal length was detected between wild type controls and *lin-17*, *lin-44* and *mig-14* mutants (Fig. 5C). This suggests that the

initial growth is not affected in the mutants but rather that these mutants miss a signal determining the final position of the canal in later larval stages. Simultaneous loss of *lin-17* and *sel-5* led to a partial rescue of the *lin-17* phenotype (Fig. 5B). Similar effect was observed in *lin-44; sel-5* double mutants (Fig. 5B). Analysis of a *lin-17; sel-5 vps-29* triple mutant was not possible as such combination was lethal. These data indicate that *sel-5* is required for the initial growth of the excretory canals and the LIN-44/Wnt signal acting through LIN-17/Frizzled receptor is required at a later stage to terminate excretory canal extension.

SEL-5 and VPS-29 genetically interact with MIG-10/Lamellipodin to control excretory canal outgrowth

So far, the most studied pathway regulating excretory canal outgrowth is the one involving UNC-53, the orthologue of mammalian Neuron Navigator 2 (Nav2), ABI-1 (Abelson-interactor protein-1) (Hedgecock et al., 1987; Stringham et al., 2002; Schmidt et al., 2009) and the Lamellipodin orthologue MIG-10 (Manser and Wood, 1990; Manser et al., 1997). All three proteins act in the same pathway for excretory canal outgrowth, possibly by affecting the cytoskeleton (McShea et al., 2013). However, it is not yet known from which membrane receptor and outside cue these proteins receive the guidance signal (Marcus-Gueret et al., 2012). To understand the relationship between *sel-5* and *vps-29* and the UNC-53/ABI-1/MIG-10 pathway we decided to analyse their genetic interaction. We chose *mig-10(ct41)* allele for testing as it displays the strongest excretory canal shortening phenotype and is predicted to act early in the pathway (McShea et al., 2013). In *sel-5 mig-10* and *mig-10 vps-29* animals we did not observe any enhancement of the posterior canal shortening compared to *mig-10* single mutants (Fig. 6A). Triple *sel-5 mig-10 vps-29* mutants were not viable. To overcome this obstacle, we performed RNAi against *vps-29* or *vps-35* in *sel-5 mig-10* double mutants. Both RNAi treatments resulted in more severe truncation of the posterior canals compared to the

controls. In *vps-35* RNAi treated animals 76% of the posterior canals did not initiate their extension at all (Fig. 6A,B). These findings suggest that SEL-5 and the retromer could act in parallel with MIG-10 to control excretory canal extension.

Taken together, our findings demonstrate that the length of the excretory cell canals is coordinated by several mechanisms, summarized in a model in Fig. 6C. First, the active outgrowth of the posterior canals is simultaneously controlled by *sel-5*, retromer and the *mig-10* pathway, possibly with a minor contribution from *cwn-1*, *cwn-2* and *cfz-2*. After reaching the proper length, further canal extension is inhibited by signalling through *lin-44* and *lin-17*. The exact wiring and crosstalk among these players in defining excretory canal length will require further investigation.

Discussion

The NAK family kinase AAK1 has recently been added to the long list of Wnt signalling regulators (Agajanian et al., 2019), acting at the level of LRP6 endocytosis. In the present study we probed the role of *C. elegans* AAK1 orthologue SEL-5 in Wnt signalling and we uncovered its requirement for Wnt dependent QL neuroblast daughter cell migration. Furthermore, we also unveiled that SEL-5 is required during the outgrowth of the excretory canal cell prior to a Wnt dependent stop signal. Importantly, in both instances the role of SEL-5 is independent of its kinase activity, defining an alternative mode of action for this kinase.

The role of SEL-5 has not been extensively studied in *C. elegans*, the only available reports uncovered the role of *sel-5* as a genetic suppressor of a constitutively active *lin-12*/Notch mutation (Tax et al., 1997; Fares and Greenwald, 1999). Information about the protein function was missing. SEL-5 shows the highest similarity to the mammalian Numb-associated kinase family members AAK1 and BMP2K (Shaye and Greenwald 2011; Sorrell et al., 2016; Kim et al., 2018). Both AAK1 and BMP2K were shown to phosphorylate the μ2 subunit of

the AP2 adaptor at position T156 and thus regulate the clathrin-mediated endocytosis (Conner and Schmid, 2002; Ricotta et al., 2002; Ramesh et al., 2021). Our findings uncovered some similarities between SEL-5 and AAK1 or BMP2K. Firstly, we show that the level of DPY-23/AP2M1 phosphorylation in *sel-5* mutants is decreased compared to controls. Secondly, the subcellular localization of SEL-5 to punctate structures proximal to the plasma membrane in oocytes and in epidermal seam cells resembles the subcellular distribution of human AAK1 (Conner and Schmid, 2002). These data support the notion that SEL-5 has a function analogous to its mammalian counterparts.

Given the established role of AAK1 in mammalian endocytosis regulation (Kadlecova et al., 2017; Agajanian et al., 2019; Wrobel et al., 2019), it was striking to see that loss of *sel-5* expression alone had no obvious developmental consequences. However, even in mammalian cells complete loss of AP2M1 T156 phosphorylation does not result in endocytosis block but only in a reduction of its efficiency (Motley et al., 2006; Wrobel et al., 2019). In cells expressing only an AP2M1T156A mutant protein the endocytosis of transferrin receptor was reduced by only 30% (Wrobel et al., 2019). We did not observe complete loss but only a partial reduction of DPY-23 phosphorylation in *sel-5* mutants. This implies that SEL-5 is not the only kinase responsible for DPY-23 phosphorylation. It also suggests that endocytosis is not inhibited but could be only partially compromised. In such case the level of ongoing endocytosis might be sufficient to support proper developmental decisions such as the direction of Q neuroblast migration. We argued that in combination with an additional insult to the intracellular trafficking machinery, in this case the retromer complex, the suboptimal function of endocytosis would manifest itself. Indeed, *sel-5 vps-29* double mutants display two highly penetrant phenotypes – the QL.d migration defect and the shortening of the excretory cell canals. Strikingly, neither of these phenotypes can be attributed to a decrease in endocytic efficiency due to lack of DPY-23 phosphorylation. Firstly, both phenotypes can be

rescued by a tissue-specific expression of a kinase-inactive SEL-5 mutant protein. Secondly, *vps-29; dpy-23(mew25)* mutants expressing only non-phosphorylatable DPY-23 do not phenocopy *sel-5 vps-29* mutants. The independence of the SEL-5 function on its kinase activity is the most striking finding of this work and to our knowledge there is no precedence for that in the mammalian AAK1 literature. Alternative mechanisms of SEL-5 function thus have to be considered. It is possible that either SEL-5 affects endocytosis by a mechanism not dependent on DPY-23 phosphorylation or that SEL-5 regulates QL.d migration and excretory cell canal extension by endocytosis-independent mechanisms. In favour of the second possibility is our finding that localization or degradation of MIG-14/Wls, the most obvious endocytic cargo candidate for QL.d migration, does not change when comparison is made between *vps-29* and *sel-5 vps-29* mutants. However, the effect of SEL-5 on a different endocytic cargo cannot be excluded. For example, EGL-20/Wnt itself could be endocytosed and SEL-5 thus could be one of the factors shaping Wnt gradient. This notion is supported by our finding that expression in both EGL-20-producing cells and in the surrounding muscle cells is necessary to fully rescue the QL migration phenotype, although so far little is known about possible EGL-20 endocytic recycling by the producing cells. In case of excretory canal extension, the putative endocytic cargo is less evident. SEL-5 could possibly regulate the turnover of guidance receptors at the plasma membrane of the growing tip of the canal. In *Drosophila*, loss of Numb-associated kinase (Nak) results in the absence or shortening of higher order dendrites and Nak has been shown to promote endocytosis of Neuroglian/L1-CAM during dendrite extension and branching (Yang et al., 2011). In *C. elegans* excretory cell, PAT-3/β1-integrin is required for canal outgrowth (Hedgecock et al., 1987). Integrins constantly cycle between the plasma membrane and intracellular compartments using various trafficking routes (Moreno-Layseca et al., 2019). Interestingly, a retromer-dependent retrograde trafficking route of unliganded β1-integrin has been described in persistently

migrating mammalian cells (Shafaq-Zadah et al., 2015). This pathway may serve to replenish the integrin pool at the leading edge of the migrating cell. Same study also pointed out the similarity in gonad migration defects caused by depletion of *vps-35*, *ina-1*/α-integrin and *pat-3* in *C. elegans* (Lee et al., 2001; Shafaq-Zadah et al., 2015), suggesting that such retrograde integrin trafficking pathway may not be restricted to mammalian cells. The canal shortening phenotype is only observed after simultaneous loss of both *sel-5* and *vps-29*, which suggests that SEL-5 and the retromer act in parallel. For example, SEL-5 could stimulate integrin endocytosis at the tip of the growing canal while retromer could secure the delivery of new integrin molecules to the growing tip.

Possible mechanism how SEL-5 could affect endocytosis independently of DPY-23 phosphorylation follows from the finding, that SEL-5 physically interacted with REPS-1 protein in a yeast-two-hybrid assay (Tsushima et al., 2013). REPS-1 is an orthologue of mammalian REPS1 (RALBP1-associated Eps Domain-containing 1), an Eps homology containing protein known to interact with RALBP1 (RalA-binding protein 1) (Yamaguchi at al., 1997). RALBP1 is an effector of Ral GTPase that can interact with the μ2 subunit of AP2 and regulate endocytosis (Jullien-Flores et al., 2000). Importantly, human AAK1 interacted with both RALBP1 and REPS1 in several high-throughput mass spectrometry analyses (Huttlin et al., 2017; Huttlin et al., 2021; Cho et al., 2022; Golkowski et al., 2023). SEL-5 thus could possibly regulate AP2 complex indirectly via interaction with the REPS1-RALBP1 complex.

Searching for possible endocytosis-independent mechanism of SEL-5 activity is complicated by the fact that while in the case of QL.d migration SEL-5 function is cell-nonautonomous, cell-autonomous expression of SEL-5 is sufficient to rescue the *sel-5 vps-29* excretory canal extension defect. This suggests that more than one mechanism might exist. One possibility common for both phenotypes comes from recent studies in mammalian cells. BMP2K has

been shown to localize to the early secretory compartment and to regulate COPII coat assemblies (Cendrowski et al., 2020). SEL-5 thus could possibly affect Wnt secretion in case of QL.d migration or new guidance receptor delivery to the plasma membrane in case of the excretory canals. Interestingly, REPS1 and RALBP1 were recently implicated also in regulation of exocytosis and knock-down of either of them reduced neurite outgrowth in cultured neuronal cells (Wang et al., 2023). SEL-5 interaction with REPS-1 thus could be the key to the mechanism of SEL-5 action. Our data so far cannot discriminate among the above outlined possibilities and more experiments will be required to establish how SEL-5 exerts its function. The biggest question to answer will be how it does so independently of its kinase activity.

Apart from the role of SEL-5 and the retromer complex in excretory cell canal extension, we have also uncovered a significant contribution of Wnt pathway components in defining excretory canal length. The role of Wnt signalling in the outgrowth of the excretory canals has been suggested (Sundaram and Buechner, 2016), however the only evidence came from the early observation that canals overgrow in *lin-17* mutants (Hedgecock et al., 1987) and that erroneous canal branching is observed in *axl-1*/Axin-like mutants (Oosterveen et al., 2007). More recently, it has been shown that loss of PLR-1, a transmembrane E3 ubiquitin ligase, results in excretory canal shortening (Bhatt et al., 2015). PLR-1 is responsible for internalization of Frizzled receptors from the cell surface (Moffat et al., 2014). However, direct link between PLR-1 function in the excretory cell and Wnt signalling has not been established. Our analysis of single and double Wnt mutants revealed that no single or double combination tested results in pronounced shortening of the excretory canals. This suggests that Wnts do not act as major attractive cues for excretory cell outgrowth. However, it cannot be excluded that several Wnts act redundantly and only simultaneous loss of more than two Wnts would be necessary to observe canal shortening. Interestingly, excretory canals in *lin-44*

mutants grew past the normal stopping point at the level of the rectum, similar to the canals in *lin-17* mutants. LIN-44 together with its receptor LIN-17 thus seems to act as a repulsive or stop signal defining the final position of the tip of the canal. Similar role of LIN-44/LIN-17 complex has been described in case of a posterior axon of *C. elegans* GABAergic DD6 motor neuron (Maro et al., 2009). In this instance EGL-20 acts also as a repellent as simultaneous loss of *lin-44* and *egl-20* expression results in more severe posterior overgrowth of the axon. In case of the excretory canal LIN-44 is the sole repelling cue. LIN-44 has also been suggested to act as a repellent in case of several tail neurons including the PLM touch receptor neuron, ALN and PLN neurons (Zheng et al., 2015). Loss of *lin-44* or *lin-17* expression promoted outgrowth of the posterior neurites of these bipolar neurons implicating that in wild type animals LIN-44 serves as a repulsive cue.

Taken together, we have uncovered cooperation between *C. elegans* orthologue of AAK1 kinase, SEL-5, and the retromer complex in regulating cell migration and cell outgrowth, and we have also outlined the engagement of Wnt pathway components in defining the length of the excretory cell canals. The surprising independence of SEL-5 function on its kinase activity opens a new path for investigation with high relevance also for mammalian biology. AAK1 has been proposed as a potential drug target for treating various neurological disorders and preventing viral entry, where the kinase activity is the target for inhibition (Martinez-Gualda et al., 2021; Xin et al., 2023). In light of our findings, the non-enzymatic activities of AAK1 should also be taken into account.

Materials and methods

Caenorhabditis elegans strains and culture

Standard methods of cultivation, manipulation and genetics of *C. elegans* were used as described previously (Brenner 1974). Bristol N2 strain was used as wild type. Other strains, extrachromososmal and integrated arrays used in this study:

LGI: *pry-1(mu38)* (Maloof et al, 1999), *lin-17(n671)* (Brenner 1974), *lin-44(n1792)* (Herman and Horvitz, 1994), *mig-1(e1787*) (Brenner 1974)

LGII: *cwn-1(ok546), dsh-1(ok1445), mig-14(mu71)* (Harris et al., 1996), *muIs32* [*Pmec-7::gfp; lin-15(+)*] (Ch'ng et al, 2003), *huSi2* [P*mig-14::mig-14::gfp*], *mig-5(cp385[mNG-GLO^AID::mig-5])* (Heppert et al., 2018)

LGIII: *sel-5(ok363), sel-5(ok149), vps-29(tm1320), sIs10089* (McKay et al., 2003)

LGIV: *egl-20(n585)* (Harris et al., 1996), *cwn-2(ok895)*

LGV: *muIs35* [*Pmec-7::gfp; lin-15(+)*] (Ch'ng et al, 2003), *cfz-2(ok1201)*

LGX: *dpy-23(mew25)*(G. Hollopeter and G. Beacham, unpublished), *kyIs4* [*Pceh-23::unc-76::gfp + lin-15(+)*] (Zallen et al., 1999)

Molecular biology, germline transformation and RNA interference

Total RNA was isolated using the TRIzol™ reagent (cat.# 15596026, ThermoFisher Scientific) from a mixed stage population of *C. elegans* N2 strain collected from a single 9 cm NGM plate. cDNA was transcribed from total RNA using SuperScript™ III Reverse Transcriptase (cat.# 18080093, ThermoFisher Scientific) and an oligo(dT) primer. Full-length *sel-5* (isoform a), *vps-29* (isoform a) or *dpy-23* (isoform b) cDNA was PCR-amplified using gene-specific primers. PCR products were cloned into pJet1.2/blunt vector (cat.# K1232, ThermoFisher Scientific) and sequenced. Same procedure was applied to clone truncated *sel-5* cDNA from *sel-5(ok363)* and *sel-5(ok149)* mutant animals. Two- or three-fragment Gibson

assembly (Gibson et al., 2009) was employed to construct tissue-specific gene expression vectors. For that, 524 bp of *col-10* promoter sequence, 600 bp of *eft-3* promoter sequence, 4419 bp of *egl-20* promoter sequence, 2896 bp of *hlh-1* promoter sequence, 3410 bp of *pgp-12* promoter sequence and 1629 bp of *wrt-2* promoter sequence were PCR-amplified from N2 genomic DNA, cDNAs were amplified from the corresponding pJet1.2 vectors and pPD95.81 (a gift from Andrew Fire (Addgene plasmid # 1497 ; http://n2t.net/addgene:1497 ; RRID:Addgene_1497)) was a source of backbone and GFP sequences. Fragments were assembled in the desired combinations and correct assembly was verified by sequencing. SEL-5 was tagged with GFP at its N-terminus, VPS-29 and DPY-23 were tagged at their C-termini. Point mutations were introduced into *sel-5* and *dpy-23* sequences using the QuikChange Site-directed Mutagenesis kit (Agilent). Transcriptional reporter P*pgp-12::gfp* was created by inserting 3410 bp of *pgp-12* promoter upstream of GFP in pPD95.81. To create extrachromosomal arrays constructs were microinjected into distal gonads of young adults using inverted microscope Leica DMi8 equipped with DIC filters and microinjection system InjectMan® 4 and FemtoJet® 4i (Eppendorf). Microinjection mixtures contained 10 ng/µL of the plasmid of interest, 5 ng/µL P*myo-2::tdTomato* as a co-injection marker and 135 ng/µL pBluescript as a carrier DNA.

CRISPR/Cas9 SEC knock-in method (Dickinson et al., 2015) was used to generate GFP tagged endogenous *sel-5* locus and performed virtually as described (Dickinson et al., 2015 and http://wormcas9hr.weebly.com/protocols.html). 647 bp upstream of *sel-5* ATG (5' homology arm) and 558 bp *sel-5* genomic sequence starting from ATG (3' homology arm) were PCR-amplified from N2 genomic DNA with primers harbouring overhangs for Gibson assembly with the pDD282 vector (Dickinson et al., 2013) (a gift from Bob Goldstein (Addgene plasmid # 66823; http://n2t.net/addgene:66823; RRID:Addgene_66823)) and assembled with pDD282 digested with ClaI and SpeI. Sequence

GCTGAAAAGCCCTAGAGGCA was inserted into pDD162 vector for sgRNA expression (Dickonson et al., 2013) (pDD162 was a gift from Bob Goldstein (Addgene plasmid # 47549; http://n2t.net/addgene:47549 ; RRID:Addgene_47549)). Injection was performed as described above, injection mix contained 10 ng/µl pDD282 with homology arms, 50 ng/µl pDD162 with corresponding sgRNA sequence, 5 ng/µl P*myo-2::tdTomato*. Line expressing P*sel-5::gfp* was first established, several L1 animals were then exposed to a heat shock for 4 hours at 34°C to excise the selection SEC cassette and create a P*sel-5::gfp::sel-5* knock-in line.

RNA interference experiments were conducted by feeding using bacterial strains from the Ahringer library (Kamath et al. 2003). L4 larvae were transferred to RNAi plates with the desired bacterial clones and the effect of RNAi was assessed in the next generation after 3-4 days at 20°C.

Protein isolation and Western blotting

For MIG-14::GFP detection, gravid hermaphrodites were subjected to hypochlorite treatment and released embryos were left to hatch overnight in M9 buffer. Larvae were collected and washed twice in M9 buffer. Pelleted larvae were then resuspended in TX-114 buffer (25 mM Tris–HCl pH 7.5, 150 mM NaCl, 0.5 mM CaCl2, 1% TX-114 and cOmplete® protease inhibitors (Roche)), snap frozen and then ground in liquid nitrogen. Thawed lysates were centrifuged at 20,800 g for 30 minutes at 4°C, mixed with Laemmli sample buffer, separated on 8% SDS–PAGE and transferred onto Amersham™ Protran® Premium Western blotting nitrocellulose membrane. GFP was detected with monoclonal anti-GFP antibody (cat.# 11814460001, Roche) and equal loading was assessed by staining with monoclonal anti α-tubulin antibody (cat. # T9026, Sigma Aldrich). Secondary goat anti-mouse HRP-conjugated antibody (cat.# 115-035-146, Jackson Immuno-Research Laboratories) and WesternBright ECL HRP substrate (Advansta) were used to visualize the signal. Images of membranes were

taken on ImageQuant (LAS4000) and Fiji Gels plug-in was used for subsequent densitometric analysis. For endogenous phosphorylated DPY-23 and DPY-23::GFP detection, 200 L4 larvae or young adults positive for DPY-23::GFP were collected into M9 buffer for each analysed strain. Animals were washed once with M9 buffer and two times with M9 buffer with 0,001% Triton X-100. 33 µL of animal pellet in M9/0.001% Triton X-100 was mixed with 33 µL of 4X Laemmli buffer, 4 µL of 20x PhosStop® phosphatase inhibitors (Roche), 4 µL of 20x cOmplete® protease inhibitors (Roche) and 1,6 µL of 1 M DTT. Samples were snap frozen in liquid nitrogen, thawed on ice, and sonicated with 2x 10 pulses at 0.8 amplitude, 0.85 duty cycle with UP50H ultrasound processor (Hielscher). Samples were heated to 99 °C for 5 minutes and centrifuged at 20,000 g for 10 minutes. 20 µL of each sample were loaded on 9% SDS-PAGE, separated and further processed as above using anti-GFP and anti-phosphoAP2M1 (cat. # ab109397, Abcam) antibodies.

Caenorhabditis elegans **phenotypes, microscopy and statistical analyses**

Final position of QL.paa (PVM – QL.d phenotype), polarity of ALM and PLM neurons was assessed in L4 larvae carrying transgene *muIs32* or *muIs35*. PVM migration was scored as defective when PVM was located anteriorly to the posterior edge of the vulva. ALM polarity was scored as defective when bipolar or reversed neurites were observed. CAN neurons were visualized with *kyIs4* transgene and their position relative to V3 seam cell was scored. CAN positioned anterior to V3 was scored as displaced. For DiI staining, L3-L4 well-fed animals were washed from a plate with M9 buffer and incubated for three hours in 10 µg/ml DiI solution (D282, ThermoFisher Scientific, dissolved to 2 mg/ml stock solution in dimethylformamide). Animals were then washed three times in M9 buffer and directly observed. Excretory cell canals lengths were scored in L4 or young adult animals carrying integrated P*pgp-12::gfp* transgene (*sIs10089*) or P*pgp-12::gfp* expressed from an

extrachromosomal array (*mamEx11 or mamEx29*). Posterior canals were scored as wild type when they reached region between the inner edge of posterior gonadal turn and the rectum. Shortened canal phenotype was graded according to the region within worm body the canal reached and following landmarks were used for each category: 0 – excretory canal missing entirely or reaching the inner edge of anterior gonadal turn, 1 – canal reaching anterior spermatheca, 2 – canal reaching vulva, 3 – canal reaching posterior spermatheca, 4 – canal reaching inner edge of posterior gonadal turn, 5 – canal reaching rectum (wild type). Canals which overgrew the rectum and reached the tail tip were scored as 6. Anterior excretory cell canals were measured and their length normalized to measured distance between the posterior edge of the pharynx and the nose tip. Larval excretory cell posterior canals were measured at four developmental stages (hatch, 4, 8 and 24 h after hatching) and normalized to animal body length. For microscopy imaging worms were anesthetised either with 10 mM sodium azide or 1 mM levamisol and mounted on 3% agarose pads. Images were taken on inverted microscope Leica DM6. For confocal imaging Zeiss LSM880 confocal microscope was used. Images were processed with Fiji image processing package (Schindelin et al., 2012). Statistical analyses were performed either in GraphPad Prism or in Excel equipped with the Real Statistics Resource Pack software (Release 7.6). Copyright (2013 – 2021) Charles Zaiontz, www.real-statistics.com.

Acknowledgements

We thank Gunther Hollopeter and Gwendolyn Beacham (Cornell University, USA) for sharing the *apm-2(mew25)* allele. We thank Jan Mašek and Teije C. Middelkoop for critically reading the manuscript. Some strains were provided by the Caenorhabditis Genetics Center (CGC) which is supported by the National Institutes of Health - Office of Research Infrastructure Programs (P40 OD010440). This work was funded by Charles University Grant

Agency grant 1446218/2018 to F.K. and by Charles University programme SVV 260559. Microscopy was performed in the Vinicna Microscopy Core Facility co-financed by the Czech-BioImaging large RI project LM2023050. Computational resources were supplied by the project "e-Infrastruktura CZ" (e-INFRA LM2018140) provided within the program Projects of Large Research, Development and Innovations Infrastructures

References

Ackley, B. D. (2014). Wnt-signaling and planar cell polarity genes regulate axon guidance along the anteroposterior axis in C. elegans. *Developmental Neurobiology*, *74*(8), 781–796. https://doi.org/10.1002/dneu.22146

Agajanian, M. J., Walker, M. P., Axtman, A. D., Ruela-de-Sousa, R. R., Serafin, D. S., Rabinowitz, A. D., Graham, D. M., Ryan, M. B., Tamir, T., Nakamichi, Y., Zuercher, W. J., & Major, M. B. (2019). WNT Activates the AAK1 Kinase to Promote Clathrin-Mediated Endocytosis of LRP6 and Establish a Negative Feedback Loop. *Cell Reports*, *26*(1), 79-93.e8. https://doi.org/10.1016/j.celrep.2018.12.023

Albrecht, L. V., Tejeda-Muñoz, N., & de Robertis, E. M. (2021). Cell Biology of Canonical Wnt Signaling. In *Annual Review of Cell and Developmental Biology* (Vol. 37). https://doi.org/10.1146/annurev-cellbio-120319-023657

Aspöck, G., Kagoshima, H., Niklaus, G., & Bürglin, T. R. (1999). Caenorhabditis elegans has scores of hedgehog-related genes: Sequence and expression analysis. *Genome Research*, *9*(10), 909–923. https://doi.org/10.1101/gr.9.10.909

Bänziger, C., Soldini, D., Schütt, C., Zipperlen, P., Hausmann, G., & Basler, K. (2006). Wntless, a Conserved Membrane Protein Dedicated to the Secretion of Wnt Proteins from Signaling Cells. *Cell*, *125*(3), 509–522. https://doi.org/10.1016/j.cell.2006.02.049

Bartscherer, K., Pelte, N., Ingelfinger, D., & Boutros, M. (2006). Secretion of Wnt Ligands Requires Evi, a Conserved Transmembrane Protein. *Cell*, *125*(3), 523–533. https://doi.org/10.1016/j.cell.2006.04.009

Belenkaya, T. Y., Wu, Y., Tang, X., Zhou, B., Cheng, L., Sharma, Y. V., Yan, D., Selva, E. M., & Lin, X. (2008). The Retromer Complex Influences Wnt Secretion by Recycling Wntless from Endosomes to the Trans-Golgi Network. *Developmental Cell*, *14*(1), 120–131. https://doi.org/10.1016/j.devcel.2007.12.003

Bhat, J. M., Pan, J., & Hutter, H. (2015). PLR-1, a putative E3 ubiquitin ligase, controls cell polarity and axonal extensions in C. elegans. *Developmental Biology*, *398*(1), 44–56. https://doi.org/10.1016/j.ydbio.2014.11.008

Brenner, S. (1974). The genetics of Caenorhabditis elegans. *Genetics*, 77(1), 71-94. https://doi.org/10.1093/genetics/77.1.71

Buechner, M., Hall, D. H., Bhatt, H., & Hedgecock, E. M. (1999). Cystic canal mutants in Caenorhabditis elegans are defective in the apical membrane domain of the renal (excretory) cell. *Developmental Biology*, *214*(1), 227–241. https://doi.org/10.1006/dbio.1999.9398

Cendrowski, J., Kaczmarek, M., Mazur, M., Kuzmicz-Kowalska, K., Jastrzebski, K., Brewinska-Olchowik, M., Kominek, A., Piwocka, K., & Miaczynska, M. (2020). Splicing variation of bmp2k balances abundance of copii assemblies and autophagic degradation in erythroid cells. *ELife*, *9*, 1–26. https://doi.org/10.7554/ELIFE.58504

Ch'ng, Q., Williams, L., Lie, Y. S., Sym, M., Whangbo, J., & Kenyon, C. (2003). Identification of genes that regulate a left-right asymmetric neuronal migration in Caenorhabditis elegans. *Genetics*, *164*(4), 1355–1367. https://doi.org/10.1093/genetics/164.4.1355

Cho, N. H., Cheveralls, K. C., Brunner, A. D., Kim, K., Michaelis, A. C., Raghavan, P., Kobayashi, H., Savy, L., Li, J. Y., Canaj, H., Kim, J.Y.S., Stewart, E. M., Gnann, C., McCarthy, F., Cabrera, J. P., Brunetti, R. M., Chhun, B. B., Dingle, G., Hein, M.Y., Huang, B., Mehta, S. B., Weissman, J. S., Gómez-Sjöberg, R., Itzha, D. N., Royer, L. A., Mann, M., & Leonetti, M. D. (2022) OpenCell: Endogenous tagging for the cartography of human cellular organization. *Science*, 375(6585):eabi6983. https://doi: 10.1126/science.abi6983

Colozza, G., & Koo, B.-K. (2021). Ub and Dub of RNF43/ZNRF3 in the WNT signalling pathway. *EMBO Reports*, *22*(5). https://doi.org/10.15252/embr.202152970

Conner, S. D., & Schmid, S. L. (2002). Identification of an adaptor-associated kinase, AAK1, as a regulator of clathrin-mediated endocytosis. *Journal of Cell Biology*, *156*(5), 921–929. https://doi.org/10.1083/jcb.200108123

Coudreuse, D. Y. M., Roël, G., Betist, M. C., Destrée, O., & Korswagen, H. C. (2006). Wnt gradient formation requires retromer function in Wnt-producing cells. *Science*, *312*(5775), 921–924. https://doi.org/10.1126/science.1124856

Dickinson, D. J., Ward, J. D., Reiner, D. J., & Goldstein, B. (2013). Engineering the Caenorhabditis elegans genome using Cas9-triggered homologous recombination. *Nature Methods*, 10(10), 1028-1034. https://doi.org/10.1038/nmeth.2641

Dickinson, D. J., Pani, A. M., Heppert, J. K., Higgins, C. D., & Goldstein, B. (2015). Streamlined genome engineering with a self-excising drug selection cassette. *Genetics*, *200*(4), 1035–1049. https://doi.org/10.1534/genetics.115.178335

Fares, H., & Greenwald, I. (1999). SEL-5, a serine/threonine kinase that facilitates lin-12 activity in Caenorhabditis elegans. *Genetics*, *153*(4), 1641–1654. https://doi.org/10.1093/genetics/153.4.1641

Franch-Marro, X., Wendler, F., Guidato, S., Griffith, J., Baena-Lopez, A., Itasaki, N., Maurice, M. M., & Vincent, J.-P. (2008). Wingless secretion requires endosome-to-Golgi retrieval of Wntless/Evi/ Sprinter by the retromer complex. *Nature Cell Biology*, *10*(2), 170–177. https://doi.org/10.1038/ncb1678

Fujita, M., Hawkinson, D., King, K. V., Hall, D. H., Sakamoto, H., & Buechner, M. (2003). The role of the ELAV homologue EXC-7 in the development of the Caenorhabditis elegans excretory canals. *Developmental Biology*, *256*(2), 290–301. https://doi.org/10.1016/S0012-1606(03)00040-X

Gibson, D. G., Young, L., Chuang, R.-Y., Venter, J. C., Hutchison, C. A., & Smith, H. O. (2009). Enzymatic assembly of DNA molecules up to several hundred kilobases. *Nature Methods*, *6*(5), 343–345. https://doi.org/10.1038/nmeth.1318

Golkowski, M., Lius, A., Sapre, T., Lau, H. T., Moreno, T., Maly, D.J, & Ong, S. E. (2023). Multiplexed kinase interactome profiling quantifies cellular network activity and plasticity. *Molecular Cell*, 83(5), 803-818.e8. https://doi.org/10.1016/j.molcel.2023.01.015

Goodman, R. M., Thombre, S., Firtina, Z., Gray, D., Betts, D., Roebuck, J., Spana, E. P., & Selva, E. M. (2006). Sprinter: A novel transmembrane protein required for Wg secretion and signaling. *Development*, *133*(24), 4901–4911. https://doi.org/10.1242/dev.02674

Groenendyk, J., & Michalak, M. (2011). A Genome-Wide siRNA Screen Identifies Novel Phospho-enzymes Affecting Wnt/β-Catenin Signaling in Mouse Embryonic Stem Cells. *Stem Cell Reviews and Reports*, *7*(4), 910–926. https://doi.org/10.1007/s12015-011-9265-3

Gupta-Rossi, N., Ortica, S., Meas-Yedid, V., Heuss, S., Moretti, J., Olivo-Marin, J.-C., & Israël, A. (2011). The adaptor-associated kinase 1, AAK1, is a positive regulator of the notch pathway. *Journal of Biological Chemistry*, *286*(21), 18720–18730. https://doi.org/10.1074/jbc.M110.190769

Harfe, B. D., Branda, C. S., Krause, M., Stern, M. J., & Fire, A. (1998). MyoD and the specification of muscle and non-muscle fates during postembryonic development of the C. elegans mesoderm. *Development*, *125*(13), 2479–2488. https://doi.org/10.1242/dev.125.13.2479

Harris, J., Honigberg, L., Robinson, N., & Kenyon, C. (1996). Neuronal cell migration in C. elegans: Regulation of Hox gene expression and cell position. *Development*, *122*(10), 3117–3131. https://doi.org/10.1242/dev.122.10.3117

Harterink, M., Kim, D. H., Middelkoop, T. C., Doan, T. D., van Oudenaarden, A., & Korswagen, H. C. (2011). Neuroblast migration along the anteroposterior axis of C. elegans is controlled by opposing gradients of Wnts and a secreted Frizzled-related protein. *Development*, *138*(14), 2915–2924. https://doi.org/10.1242/dev.064733

Hedgecock, E. M., Culotti, J. G., Hall, D. H., & Stern, B. D. (1987). Genetics of cell and axon migrations in Caenorhabditis elegans. *Development*, *100*(3), 365–382. https://doi.org/10.1242/dev.100.3.365

Heppert, J. K., Pani, A. M., Roberts, A. M., Dickinson, D. J., & Goldstein, B. (2018). A CRISPR tagging-based screen reveals localized players in wnt-directed asymmetric cell division. *Genetics*, *208*(3), 1147–1164. https://doi.org/10.1534/genetics.117.300487

Herman, M. A., & Robert Horvitz, H. (1994). The Caenorhabditis elegans gene lin-44 controls the polarity of asymmetric cell divisions. *Development*, *120*(5), 1035–1047. https://doi.org/10.1242/dev.120.5.1035

Herman, M. A., Vassilieva, L. L., Horvitz, H. R., Shaw, J. E., & Herman, R. K. (1995). The C. elegans gene lin-44, which controls the polarity of certain asymmetric cell divisions, encodes a Wnt protein and acts cell nonautonomously. *Cell*, *83*(1), 101–110. https://doi.org/10.1016/0092-8674(95)90238-4

Hilliard, M. A., & Bargmann, C. I. (2006). Wnt signals and Frizzled activity orient anterior-posterior axon outgrowth in C. elegans. *Developmental Cell*, *10*(3), 379–390. https://doi.org/10.1016/j.devcel.2006.01.013

Hollopeter, G., Lange, J. J., Zhang, Y., Vu, T. N., Gu, M., Ailion, M., Lambie, E. J., Slaughter, B. D., Unruh, J. R., Florens, L., Florens, L., & Jorgensen, E. M. (2014). The membrane-associated proteins FCHo and SGIP are allosteric activators of the AP2 clathrin adaptor complex. *ELife*, *3*. https://doi.org/10.7554/eLife.03648

Hutter, H. (2019). Formation of longitudinal axon pathways in Caenorhabditis elegans. *Seminars in Cell and Developmental Biology*, *85*, 60–70. https://doi.org/10.1016/j.semcdb.2017.11.015

Huttlin, E. L., Bruckner, R. J., Navarrete-Perea, J., Cannon, J. R., Baltier, K., Gebreab, F., Gygi, M. P., Thornock, A., Zarraga, G., Tam, S., Harper, J. W., & Gygi, S. P. (2021). Dual proteome-scale networks reveal cell-specific remodeling of the human interactome. *Cell*, *184*(11), 3022-3040.e28. https://doi.org/10.1016/j.cell.2021.04.011

Huttlin, E. L., Bruckner, R. J., Paulo, J. A., Cannon, J. R., Ting, L., Baltier, K., Colby, G., Gebreab, F., Gygi, M. P., Parzen, H., Gygi, S. P., & Wade Harper, J. (2017). Architecture of the human interactome defines protein communities and disease networks. *Nature*, *545*(7655), 505–509. https://doi.org/10.1038/nature22366

Jullien-Flores, V., Mahe, Y., Mirey, G., Leprince, C., Meunier-Bisceuil, B., Sorkin, A., & Camonis, J. H. (2000). RLIP76, an effector of the GTPase Ral, interactas with the AP2 complex: Involvement of the Ral pathway in receptor endocytosis. *Journal of Cell Science*, *113*(16), 2837–2844. https://doi.org/10.1242/jcs.113.16.2837

Kadlecova, Z., Spielman, S. J., Loerke, D., Mohanakrishnan, A., Reed, D. K., & Schmid, S. L. (2017). Regulation of clathrin-mediated endocytosis by hierarchical allosteric activation of AP2. *Journal of Cell Biology*, *216*(1), 167–179. https://doi.org/10.1083/jcb.201608071

Kamath, R. S., & Ahringer, J. (2003). Genome-wide RNAi screening in Caenorhabditis elegans. *Methods*, *30*(4), 313–321. https://doi.org/10.1016/S1046-2023(03)00050-1

Kim, H., & Ronai, Z. A. (2018). Rewired Notch/p53 by Numb'ing Mdm2. *Journal of Cell Biology*, *217*(2), 445–446. https://doi.org/10.1083/jcb.201712007

Krause, M., Fire, A., Harrison, S. W., Priess, J., & Weintraub, H. (1990). CeMyoD accumulation defines the body wall muscle cell fate during C. elegans embryogenesis. *Cell*, *63*(5), 907–919. https://doi.org/10.1016/0092-8674(90)90494-Y

Lee, M., Cram, E. J., Shen, B., & Schwarzbauer, J. E. (2001). Roles for βpat-3 Integrins in Development and Function of Caenorhabditis elegans Muscles and Gonads. *Journal of Biological Chemistry*, *276*(39), 36404–36410. https://doi.org/10.1074/jbc.M105795200

Liégeois, S., Benedetto, A., Michaux, G., Belliard, G., & Labouesse, M. (2007). Genes required for osmoregulation and apical secretion in Caenorhabditis elegans. *Genetics*, *175*(2), 709–724. https://doi.org/10.1534/genetics.106.066035

Lorenowicz, M. J., Macurkova, M., Harterink, M., Middelkoop, T. C., de Groot, R., Betist, M. C., & Korswagen, H. C. (2014). Inhibition of late endosomal maturation restores Wnt secretion in Caenorhabditis elegans vps-29 retromer mutants. *Cellular Signalling*, *26*(1), 19–31. https://doi.org/10.1016/j.cellsig.2013.09.013

Maloof, J. N., Whangbo, J., Harris, J. M., Jongeward, G. D., & Kenyon, C. (1999). A Wnt signaling pathway controls Hox gene expression and neuroblast migration in C. elegans. *Development*, *126*(1), 37–49. https://doi.org/10.1242/dev.126.1.37

Manser, J., Roonprapunt, C., & Margolis, B. (1997). C. elegans cell migration gene mig-10 shares similarities with a family of SH2 domain proteins and acts cell nonautonomously in excretory canal development. *Developmental Biology*, *184*(1), 150–164. https://doi.org/10.1006/dbio.1997.8516

Manser, J., & Wood, W. B. (1990). Mutations affecting embryonic cell migrations in Caenorhabditis elegans. *Developmental Genetics*, *11*(1), 49–64. https://doi.org/10.1002/dvg.1020110107

Marcus-Gueret, N., Schmidt, K. L., & Stringham, E. G. (2012). Distinct cell guidance pathways controlled by the Rac and Rho GEF domains of UNC-73/TRIO in Caenorhabditis elegans. *Genetics*, *190*(1), 129–142. https://doi.org/10.1534/genetics.111.134429

Maro, G. S., Klassen, M. P., & Shen, K. (2009). A β-catenin-dependent Wnt pathway mediates anteroposterior axon guidance in C. elegans motor neurons. *PLoS ONE*, *4*(3). https://doi.org/10.1371/journal.pone.0004690

Martinez-Gualda, B., Graus, M., Camps, A., Vanhulle, E., Saul, S., Azari, S., Nhu Tran, D. H., Vangeel, L., Chiu, W., Neyts, J., Vermeire, K., & de Jonghe, S. (2022). Synthesis and evaluation of 3-alkynyl-5-aryl-7-aza-indoles as broad-spectrum antiviral agents. *Frontiers in Chemistry*, *10*. https://doi.org/10.3389/fchem.2022.1058229

McKay, S. J., Johnsen, R., Khattra, J., Asano, J., Baillie, D. L., Chan, S., Dube, N., Fang, L., Goszczynski, B., Ha, E., Zhao, Z., & Moerman, D. G. (2003). Gene expression profiling of cells, tissues, and developmental stages of the nematode C. elegans. In *Cold Spring Harbor Symposia on Quantitative Biology* (Vol. 68). https://doi.org/10.1101/sqb.2003.68.159

McShea, M. A., Schmidt, K. L., Dubuke, M. L., Baldiga, C. E., Sullender, M. E., Reis, A. L., Zhang, S., O'Toole, S. M., Jeffers, M. C., Warden, R. M., Stringham, E. G., & Ryder, E. F. (2013). Abelson interactor-1 (ABI-1) interacts with MRL adaptor protein MIG-10 and is required in guided cell migrations and process outgrowth in C. elegans. *Developmental Biology*, *373*(1), 1–13. https://doi.org/10.1016/j.ydbio.2012.09.017

Middelkoop, T. C., & Korswagen, H. C. (2014). Development and migration of the C. elegans Q neuroblasts and their descendants. *WormBook : The Online Review of C. Elegans Biology*, 1–23. https://doi.org/10.1895/wormbook.1.173.1

Middelkoop, T. C., Williams, L., Yang, P.-T., Luchtenberg, J., Betist, M. C., Ji, N., van Oudenaarden, A., Kenyon, C., & Korswagen, H. C. (2012). The thrombospondin repeat containing protein MIG-21 controls a left-right asymmetric Wnt signaling response in migrating C. elegans neuroblasts. *Developmental Biology*, *361*(2), 338–348. https://doi.org/10.1016/j.ydbio.2011.10.029

Moffat, L. L., Robinson, R. E., Bakoulis, A., & Clark, S. G. (2014). The conserved transmembrane RING finger protein PLR-1 downregulates Wnt signaling by reducing Frizzled, Ror and Ryk cell-surface levels in C. elegans. *Development (Cambridge)*, *141*(3), 617–628. https://doi.org/10.1242/dev.101600

Moreno-Layseca, P., Icha, J., Hamidi, H., & Ivaska, J. (2019). Integrin trafficking in cells and tissues. *Nature Cell Biology*, *21*(2), 122–132. https://doi.org/10.1038/s41556-018-0223-z

Motley, A. M., Berg, N., Taylor, M. J., Sahlender, D. A., Hirst, J., Owen, D. J., & Robinson, M. S. (2006). Functional analysis of AP-2 α and μ2 subunits. *Molecular Biology of the Cell*, *17*(12), 5298–5308. https://doi.org/10.1091/mbc.E06-05-0452

Oosterveen, T., Coudreuse, D. Y. M., Yang, P.-T., Fraser, E., Bergsma, J., Dale, T. C., & Korswagen, H. C. (2007). Two functionally distinct Axin-like proteins regulate canonical Wnt signaling in C. elegans. *Developmental Biology*, *308*(2), 438–448. https://doi.org/10.1016/j.ydbio.2007.05.043

Pan, C.-L., Baum, P. D., Gu, M., Jorgensen, E. M., Clark, S. G., & Garriga, G. (2008). C. elegans AP-2 and Retromer Control Wnt Signaling by Regulating MIG-14/Wntless. *Developmental Cell*, *14*(1), 132–139. https://doi.org/10.1016/j.devcel.2007.12.001

Pan, C.-L., Howell, J. E., Clark, S. G., Hilliard, M., Cordes, S., Bargmann, C. I., & Garriga, G. (2006). Multiple Wnts and Frizzled receptors regulate anteriorly directed cell and growth cone

migrations in Caenorhabditis elegans. *Developmental Cell*, *10*(3), 367–377. https://doi.org/10.1016/j.devcel.2006.02.010

Peng, Y.-H., Yang, W.-K., Lin, W.-H., Lai, T.-T., & Chien, C.-T. (2009). Nak regulates Dlg basal localization in Drosophila salivary gland cells. *Biochemical and Biophysical Research Communications*, *382*(1), 108–113. https://doi.org/10.1016/j.bbrc.2009.02.139

Port, F., Kuster, M., Herr, P., Furger, E., Bänziger, C., Hausmann, G., & Basler, K. (2008). Wingless secretion promotes and requires retromer-dependent cycling of Wntless. *Nature Cell Biology*, *10*(2), 178–185. https://doi.org/10.1038/ncb1687

Prasad, B. C., & Clark, S. G. (2006). Wnt signaling establishes anteroposterior neuronal polarity and requires retromer in C. elegans. *Development*, *133*(9), 1757–1766. https://doi.org/10.1242/dev.02357

Ramesh, S. T., Navyasree, K. V., Sah, S., Ashok, A. B., Qathoon, N., Mohanty, S., Swain, R. K., & Umasankar, P. K. (2021). BMP2K phosphorylates AP-2 and regulates clathrin-mediated endocytosis. *Traffic*, *22*(11), 377–396. https://doi.org/10.1111/tra.12814

Rella, L., Fernandes Póvoa, E. E., & Korswagen, H. C. (2016). The Caenorhabditis elegans Q neuroblasts: A powerful system to study cell migration at single-cell resolution in vivo. *Genesis*, *54*(4), 198–211. https://doi.org/10.1002/dvg.22931

Ricotta, D., Conner, S. D., Schmid, S. L., von Figura, K., & Höning, S. (2002). Phosphorylation of the AP2 μ subunit by AAK1 mediates high affinity binding to membrane protein sorting signals. *Journal of Cell Biology*, *156*(5), 791–795. https://doi.org/10.1083/jcb.200111068

Salser, S. J., & Kenyon, C. (1992). Activation of a C. elegans Antennapedia homologue in migrating cells controls their direction of migration. *Nature*, *355*(6357), 255–258. https://doi.org/10.1038/355255a0

Schindelin, J., Arganda-Carreras, I., Frise, E., Kaynig, V., Longair, M., Pietzsch, T., Preibisch, S., Rueden, C., Saalfeld, S., Schmid, B., Tomancak, P., & Cardona, A. (2012). Fiji: An open-source platform for biological-image analysis. *Nature Methods*, *9*(7), 676–682. https://doi.org/10.1038/nmeth.2019

Schmidt, K. L., Marcus-Gueret, N., Adeleye, A., Webber, J., Baillie, D., & Stringham, E. G. (2009). The cell migration molecule UNC-53/NAV2 is linked to the ARP2/3 complex by ABI-1. *Development*, *136*(4), 563–574. https://doi.org/10.1242/dev.016816

Shafaq-Zadah, M., Gomes-Santos, C. S., Bardin, S., Maiuri, P., Maurin, M., Iranzo, J., Gautreau, A., Lamaze, C., Caswell, P., Goud, B., Goud, B., & Johannes, L. (2016). Persistent cell migration and adhesion rely on retrograde transport of β 1 integrin. *Nature Cell Biology*, *18*(1), 54–64. https://doi.org/10.1038/ncb3287

Shaye, D. D., & Greenwald, I. (2011). Ortholist: A compendium of C. elegans genes with human orthologs. *PLoS ONE*, *6*(5). https://doi.org/10.1371/journal.pone.0020085

Sherwood, D. R., & Plastino, J. (2018). Invading, leading and navigating cells in caenorhabditis elegans: Insights into cell movement in vivo. *Genetics*, *208*(1), 53–78. https://doi.org/10.1534/genetics.117.300082

Silhankova, M., & Korswagen, H. C. (2007). Migration of neuronal cells along the anterior-posterior body axis of C. elegans: Wnts are in control. *Current Opinion in Genetics and Development*, *17*(4), 320–325. https://doi.org/10.1016/j.gde.2007.05.007

Smythe, E., & Ayscough, K. R. (2003). The Ark1/Prk1 family of protein kinases. Regulators of endocytosis and the actin cytoskeleton. *EMBO Reports*, *4*(3), 246–251. https://doi.org/10.1038/sj.embor.embor776

Sorensen, E. B., & Conner, S. D. (2008). AAK1 regulates Numb function at an early step in clathrin-mediated endocytosis. *Traffic*, *9*(10), 1791–1800. https://doi.org/10.1111/j.1600-0854.2008.00790.x

Sorrell, F. J., Szklarz, M., Abdul Azeez, K. R., Elkins, J. M., & Knapp, S. (2016). Family-wide Structural Analysis of Human Numb-Associated Protein Kinases. *Structure*, *24*(3), 401–411. https://doi.org/10.1016/j.str.2015.12.015

Spencer, A. G., Orita, S., Malone, C. J., & Han, M. (2001). A RHO GTPase-mediated pathway is required during P cell migration in Caenorhabditis elegans. *Proceedings of the National Academy of Sciences of the United States of America*, *98*(23), 13132–13137. https://doi.org/10.1073/pnas.241504098

Stringham, E., Pujol, N., Vandekerckhove, J., & Bogaert, T. (2002). Unc-53 controls longitudinal migration in C. elegans. *Development*, *129*(14), 3367–3379. https://doi.org/10.1242/dev.129.14.3367

Sundaram, M. V., & Buechner, M. (2016). The caenorhabditis elegans excretory system: A model for tubulogenesis, cell fate specification, and plasticity. *Genetics*, *203*(1), 35–63. https://doi.org/10.1534/genetics.116.189357

Tax, F. E., Thomas, J. H., Ferguson, E. L., & Horvitz, H. R. (1997). Identification and characterization of genes that interact with lin-12 in Caenorhabditis elegans. *Genetics*, *147*(4), 1675–1695. https://doi.org/10.1093/genetics/147.4.1675

Tsushima, H., Malabarba, M. G., Confalonieri, S., Senic-Matuglia, F., Verhoef, L. G. G. C., Bartocci, C., D'Ario, G., Cocito, A., di Fiore, P. P., & Salcini, A. E. (2013). A Snapshot of the Physical and Functional Wiring of the Eps15 Homology Domain Network in the Nematode. *PLoS ONE*, *8*(2). https://doi.org/10.1371/journal.pone.0056383

Wang, S., Chen, X., Crisman, L., Dou, X., Winborn, C. S., Wan, C., Puscher, H., Yin, Q., Kennedy, M. J., & Shen, J. (2023). Regulation of cargo exocytosis by a Reps1-Ralbp1-RalA module. *Science Advances*, *9*(8), eade2540. https://doi.org/10.1126/sciadv.ade2540

Whangbo, J., & Kenyon, C. (1999). A Wnt signaling system that specifies two patterns of cell migration in C. elegans. *Molecular Cell*, *4*(5), 851–858. https://doi.org/10.1016/S1097-2765(00)80394-9

Wrobel, A. G., Kadlecova, Z., Kamenicky, J., Yang, J.-C., Herrmann, T., Kelly, B. T., McCoy, A. J., Evans, P. R., Martin, S., Müller, S., Honing, S., & Owen, D. J. (2019). Temporal Ordering in Endocytic Clathrin-Coated Vesicle Formation via AP2 Phosphorylation. *Developmental Cell*, *50*(4), 494-508.e11. https://doi.org/10.1016/j.devcel.2019.07.017

Wu, Y. C., Chiang, Y. C., Chou, S. H., & Pan, C. L. (2021). Wnt signalling and endocytosis: Mechanisms, controversies and implications for stress responses. *Biology of the Cell*, 113(2), 95-106. https://doi.org/10.1111/boc.202000099.

Xin, X., Wang, Y., Zhang, L., Zhang, D., Sha, L., Zhu, Z., Huang, X., Mao, W., & Zhang, J. (2023). Development and therapeutic potential of adaptor-associated kinase 1 inhibitors in human multifaceted diseases. *European Journal of Medicinal Chemistry*, 248:115102. https://doi.org/10.1016/j.ejmech.2023.115102

Yamaguchi, A., Urano, T., Goi, T., & Feig, L. A. (1997). An Eps homology (EH) domain protein that binds to the Ral-GTPase target, RalBP1. *Journal of Biological Chemistry*, *272*(50), 31230–31234. https://doi.org/10.1074/JBC.272.50.31230

Yang, P.-T., Lorenowicz, M. J., Silhankova, M., Coudreuse, D. Y. M., Betist, M. C., & Korswagen, H. C. (2008). Wnt Signaling Requires Retromer-Dependent Recycling of MIG-14/Wntless in Wnt-Producing Cells. *Developmental Cell*, *14*(1), 140–147. https://doi.org/10.1016/j.devcel.2007.12.004

Yang, W.-K., Peng, Y.-H., Li, H., Lin, H.-C., Lin, Y.-C., Lai, T.-T., Suo, H., Wang, C.-H., Lin, W.-H., Ou, C.-Y., Chang, H., & Chien, C.-T. (2011). Nak regulates localization of clathrin sites in higher-order dendrites to promote local dendrite growth. *Neuron*, *72*(2), 285–299. https://doi.org/10.1016/j.neuron.2011.08.028

Yu, J., Chia, J., Canning, C. A., Jones, C. M., Bard, F. A., & Virshup, D. M. (2014). WLS Retrograde transport to the endoplasmic reticulum during Wnt secretion. *Developmental Cell*, *29*(3), 277–291. https://doi.org/10.1016/j.devcel.2014.03.016

Zallen, J. A., Kirch, S. A., & Bargmann, C. I. (1999). Genes required for axon pathfinding and extension in the C. elegans nerve ring. *Development*, *126*(16), 3679–3692. https://doi.org/10.1242/dev.126.16.3679

Zhao, Z., Sheps, J. A., Ling, V., Fang, L. L., & Baillie, D. L. (2004). Expression analysis of ABC transporters reveals differential functions of tandemly duplicated genes in Caenorhabditis elegans. *Journal of Molecular Biology*, *344*(2), 409–417. https://doi.org/10.1016/j.jmb.2004.09.052

Zheng, C., Diaz-Cuadros, M., & Chalfie, M. (2015). Dishevelled attenuates the repelling activity of Wnt signaling during neurite outgrowth in Caenorhabditis elegans. *Proceedings of the National Academy of Sciences of the United States of America*, *112*(43), 13243–13248. https://doi.org/10.1073/pnas.1518686112

Zinovyeva, A. Y., & Forrester, W. C. (2005). The C. elegans Frizzled CFZ-2 is required for cell migration and interacts with multiple Wnt signaling pathways. *Developmental Biology*, *285*(2), 447–461. https://doi.org/10.1016/j.ydbio.2005.07.014

Zinovyeva, A. Y., Yamamoto, Y., Sawa, H., & Forrester, W. C. (2008). Complex network of Wnt signaling regulates neuronal migrations during Caenorhabditis elegans development. *Genetics*, *179*(3), 1357–1371. https://doi.org/10.1534/genetics.108.090290

Table 1. Phenotypes of *sel-5* and *vps-29* single and double mutants

Genotype	ALM (%)[a]	PLM (%)[b]	CAN (%)[c]	Dye filling (%)[d]	Fecundity (n)[e]
Wild type	0.0	0.0	0.6	0.5	280 ± 41
sel-5(ok149)	0.0	0.0	8.9	4.7	236 ± 24
sel-5(ok363)	0.0	0,0	10.9	1.0	249 ± 37
vps-29(tm1320)	0.0	0.0	2.9	4.3	221 ± 28
sel-5(ok149) vps-29	29.9	9.1	17.7	17.4	132 ± 40
sel-5(ok363) vps-29	7.2	2.8	16.3	7.1	159 ± 23

[a] % of animals with axons of one or both ALM reversed/bipolar, n > 60

[b] % of animals with axons of one or both PLM neurons reversed, n > 60

[c] % of CAN neurons located anteriorly of V3 seam cell, n > 40

[d] % of animals with one or both phasmid sensilla not dyed with DiI, n > 40

[e] average number of progeny from 5 hermaphrodites, ± s.d.

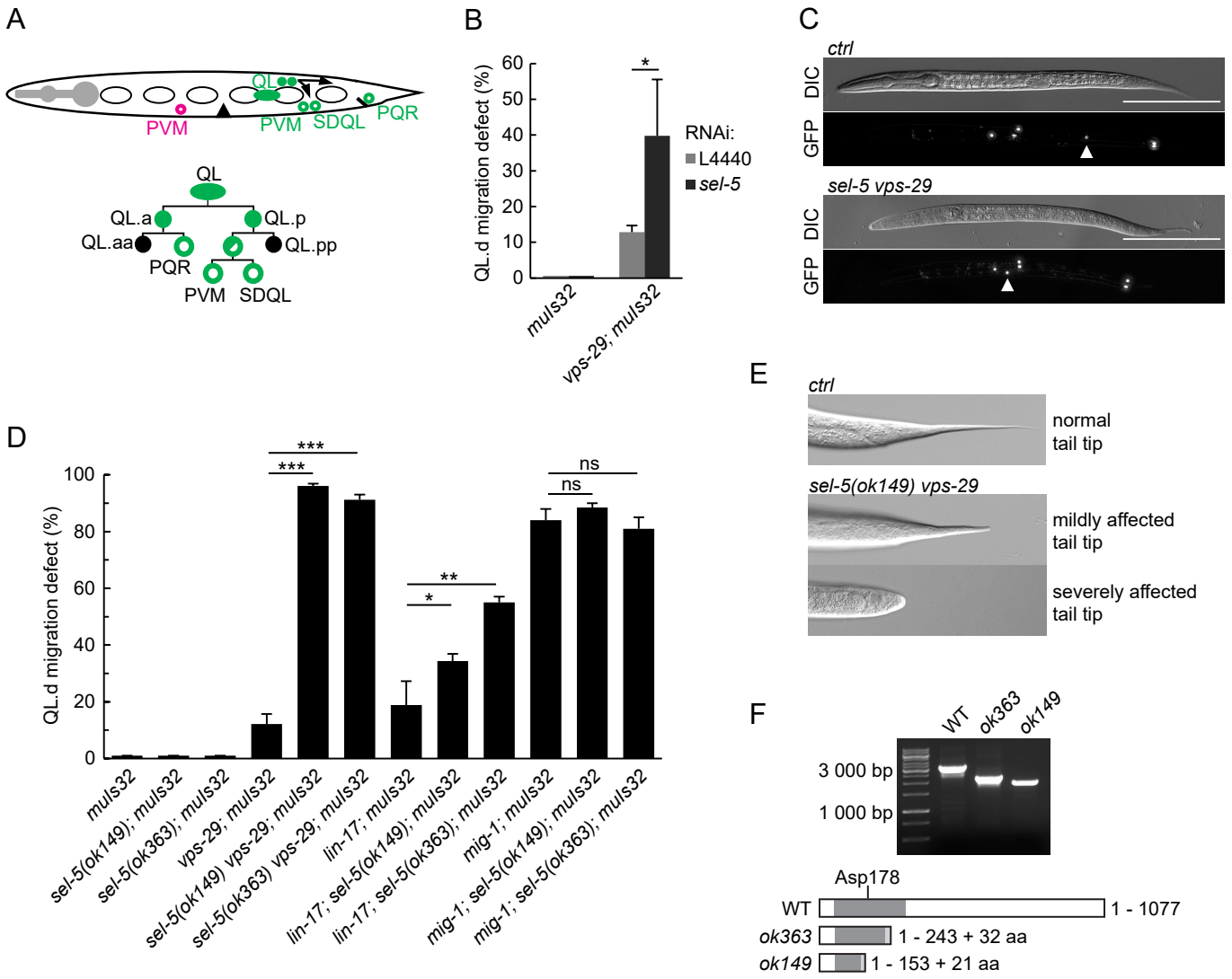

Figure 1. Loss of *sel-5* potentiates QL migration defect in retromer and Wnt pathway mutants. A) QL neuroblast lineage and a cartoon indicating the position of terminally differentiated neurons (depicted with empty circles) (adapted from Rella et al., 2016). Aberrant position of PVM neuron, as observed in QL.d migration defect, is highlighted in magenta. B) RNAi against *sel-5* increases the penetrance of *vps-29* QL.d migration defect when compared to the control (L4440) RNAi. No defect is observed in wild type background. C) PVM position in L2 larvae of control (transgene only) and *sel-5 vps-29* double mutant animals. PVM position indicated with white arrowhead, neurons visualized by expression of P*mec-7::gfp* transgene *muIs32*, scale bar represents 100 µm. D) Mutation in *sel-5* results in increased penetrance of QL.d migration defect of *vps-29* and *lin-17*, but not *mig-1* mutants. E) Examples of mild and severe alteration of tail tip morphology in *sel-5 vps-29* double mutants. F) Shortened transcripts are produced from the *sel-5* locus in both *ok363* and *ok149* alleles. Potential protein products resulting from these transcripts are depicted showing the impact of the truncation on the kinase domain (dark grey box). Extra amino acids resulting from a frameshift and thus not present in the wild type protein are also depicted (light grey box). Position of the active site is indicated. For B) and D) results are shown as mean + s.d. of at least three independent experiments, n > 150 animals in total for each strain, unpaired two-tailed Student's t-test was performed to assess the difference between the samples, * p-value < 0.05, ** p-value < 0.01, *** p-value < 0.001, ns – not significant.

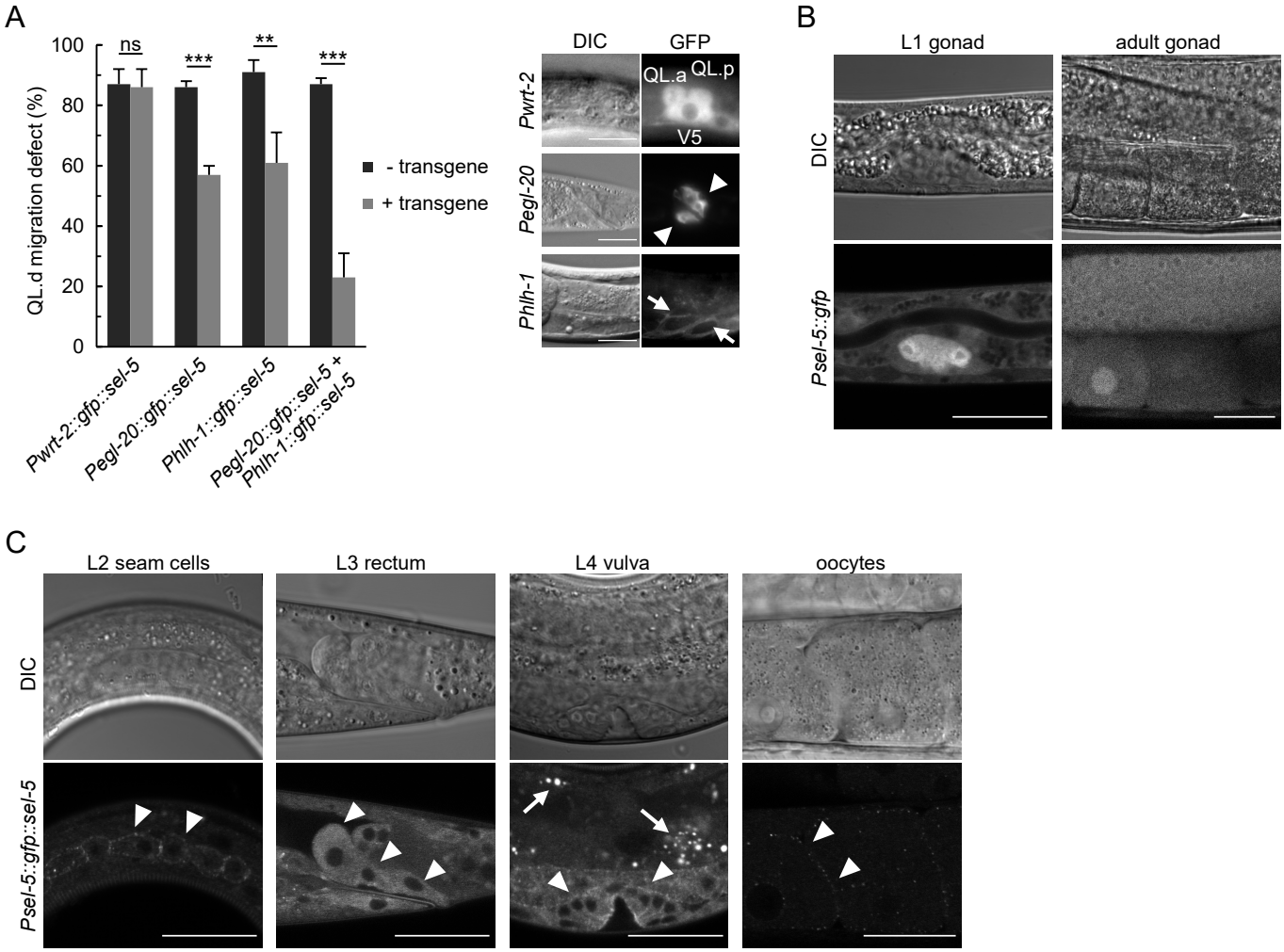

Figure 2. SEL-5 is expressed in multiple tissues and is required cell-nonautonomously for QL.d migration. A) Transgenic rescue of the QL.d migration defect. *sel-5* was expressed under the control of various promoters from an extrachromosomal array in *sel-5 vps-29; muIs32* background and the effect of such expression on QL.d migration was quantified. Comparison was made between animals carrying the transgene and their siblings which have lost the transgenic array. Expression of each transgene in the expected tissue is shown on the right. Results are shown as mean + s.d. of at least three independent experiments, n > 100 animals in total for each condition. Unpaired two-tailed Student's t-test was performed to assess the difference between the samples, ** p-value < 0.01, *** p-value < 0.001, ns – not significant. B) GFP expression driven by an endogenous *sel-5* promoter in the gonad of L1 and adult animals. C) Expression of GFP::SEL-5 fusion protein driven by endogenous *sel-5* promoter in various larval and adult tissues. Localized GFP::SEL-5 expression is indicated by white arrowheads, white arrows point to autofluorescent signal from gut granules. Scale bar represents 20 μm in A) – C).

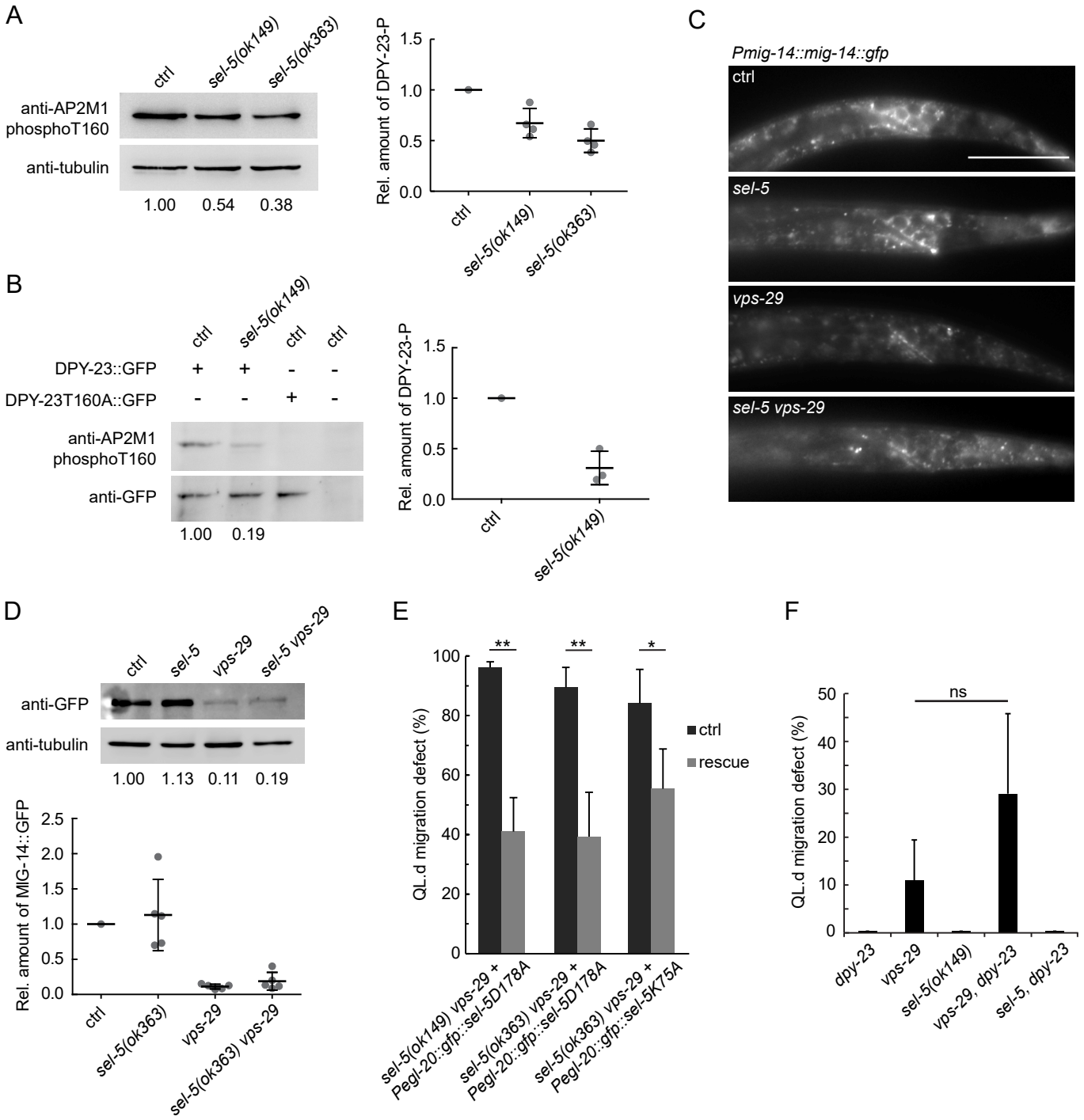

Figure 3. SEL-5 alters the phosphorylation status of DPY-23 but its kinase activity is not required for QL.d migration. A) Level of DPY-23 phosphorylation at position T160 is reduced in *sel-5* mutant animals. Phosphorylation was detected by Western blot analysis in lysates from a population of L4/young adults of indicated strains using phospho-specific antibody against human AP2M1. Band intensities were normalized to an alpha tubulin loading control and compared to the control sample (sample/control ratio indicated below each lane). Representative Western blot example is shown on the left, relative quantification of four independent experiments is shown on the right. B) Level of DPY-23::GFP phosphorylation is reduced in *sel-5* mutants. Phosphorylation at T160 of GFP tagged DPY-23 was detected by Western blot analysis in lysates from a population of L4/young adults using phospho-specific antibody against human AP2M1. Strains expressing either no GFP fusion protein or a GFP tagged DPY-23T160A mutant protein

(continued) were included as controls. Band intensities were normalized to a GFP signal intensity and compared to the control sample (DPY-23::GFP in wild type background), sample/control ratio is indicated below each lane. Representative Western blot example is shown on the left, relative quantification of three independent experiments is shown on the right. C) L2 animals expressing MIG-14::GFP from the *huSi2* transgene were imaged using confocal microscope. Posterior part of the body with Wnt expressing cells is shown. Anterior to the left, dorsal up, scale bar represents 20 μm. D) Western blot analysis of MIG-14::GFP levels expressed from a *huSi2* transgene in various mutant backgrounds. MIG-14::GFP was detected in lysates from synchronized populations of L1 larvae of the indicated strains. Band intensities were normalized to an alpha tubulin loading control and compared to the control sample (sample/-control ratio indicated below each lane). Representative Western blot example is shown on the top, relative quantification of five independent experiments is shown below. E) Transgenic rescue of the QL.d migration defect with kinase-inactive SEL-5. D178A or K75A SEL-5 mutant protein was expressed from *egl-20* promoter in *sel-5 vps-29; muIs32* mutant background from an extrachromosomal array and the QL.d migration defect was quantified in animals carrying the transgene and their siblings which have lost the transgenic array. F) The absence of DPY-23 T160 phosphorylation does not result in QL.d migration defect. The presence of *dpy-23(mew25)* allele carrying T160A substitution either alone or in combination with *sel-5* or *vps-29* does not significantly contribute to the QL.d migration defect. For E) and F) results are shown as mean + s.d. of at least three independent experiments, $n > 100$. Unpaired two-tailed Student's t-test was performed to assess the difference between the samples, * p-value < 0.05, ** p-value < 0.01, ns – not significant.

A

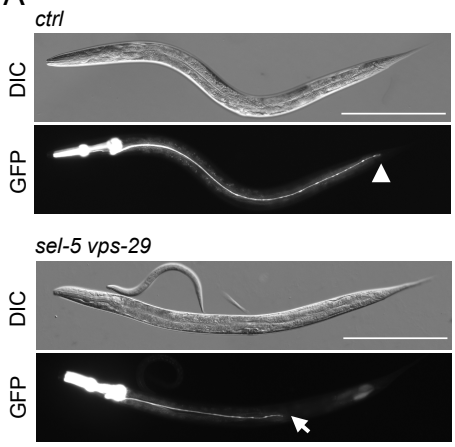

B

	0	1	2	3	4	5	6	N	p-value	versus
mamEx11	0	0	0	0	0	100	0	230		
sel-5(ok149)	0	0	0	0	5	95	0	187	0.0043	*mamEx11*
sel-5(ok363)	0	0	0	1	10	89	0	210	<0.0001	*mamEx11*
vps-29	0	0	0	0	5	95	0	220	0.0025	*mamEx11*
sel-5(ok149) vps-29	19	4	20	19	18	19	1	180	<0.0001	*sel-5(ok149)*
sel-5(ok363) vps-29	1	1	10	15	50	23	0	211	<0.0001	*sel-5(ok363)*

C

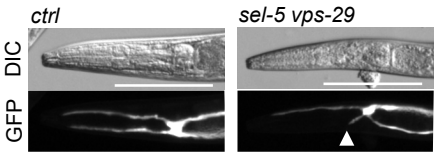

	% short	N
mamEx29	0	122
vps-29	0	84
sel-5(ok363)	0	80
sel-5(ok363) vps-29	12.5	112

D

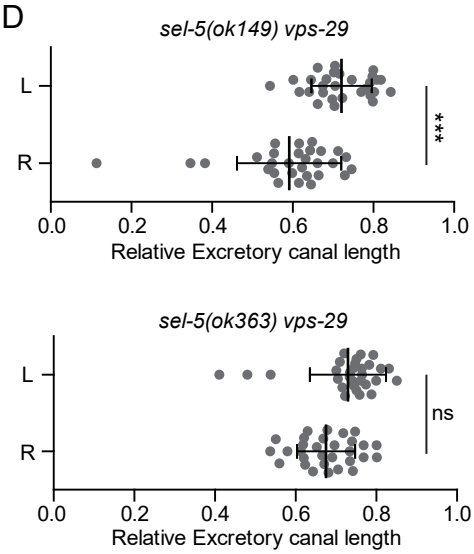

E

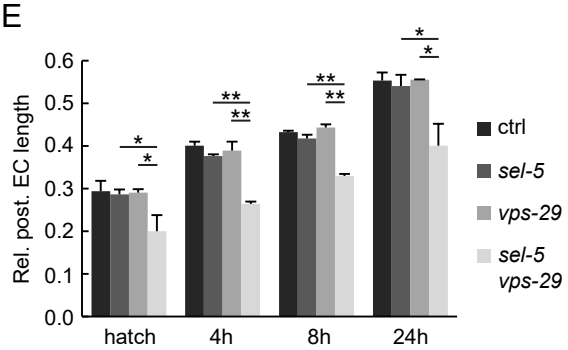

F

	0	1	2	3	4	5	6	N	p-value
sel-5(ok149); L4440 RNAi	0	0	0	0	2	97	1	376	
+ vps-35 RNAi	0	0	1	14	35	50	0	278	<0.0001
+ vps-26 RNAi	0	0	0	6	31	63	0	254	<0.0001
+ snx-1 RNAi	0	0	0	0	3	97	0	330	0.5233†
+ snx-3 RNAi	0	0	0	2	15	83	0	324	<0.0001

G

	0	1	2	3	4	5	6	N	p-value
sel-5(ok363) vps-29	7	1	7	14	22	47	2	166	
+ hlh-1p::gfp::sel-5	10	3	3	9	31	39	5	174	0.1197†
sel-5(ok363) vps-29	10	2	6	12	37	33	0	219	
+ pgp-12p::gfp::sel-5	4	0	1	3	7	83	2	169	<0.0001
sel-5(ok363) vps-29	1	1	2	7	30	59	0	180	
+ col-10p::gfp::sel-5	1	0	1	4	13	81	0	180	<0.0001
sel-5(ok149) vps-29	11	3	20	30	24	12	0	150	
+ pgp-12p::vps-29::gfp	10	2	9	13	26	40	0	169	<0.0001
sel-5(ok363) vps-29	4	1	2	11	34	48	0	158	
+ pgp-12p::gfp::sel-5D178A	1	0	1	2	10	85	0	158	<0.0001

H

	0	1	2	3	4	5	6	N	p-value
dpy-23(mew25)	0	0	0	0	0	97	3	196	
sel-5(ok149)‡	0	0	0	0	5	95	0	187	
sel-5(ok149); dpy-23(mew25)	0	0	0	0	7	93	0	182	0.4604†
vps-29‡	0	0	0	0	5	95	0	220	
vps-29; dpy-23(mew25)	0	0	0	0	4	91	5	186	0.0025

Figure 4. *sel-5* cooperates with the retromer complex to regulate the length of excretory cell canals. A) Posterior canals of the excretory cell are significantly shortened in *sel-5 vps-29* mutants. Excretory cell was visualized by P*pgp-12::gf*p expression from a *mamEx11* transgene. Scale bar represents 200 µm. B) Quantification of posterior canal outgrowth defects. The outgrowth of the posterior canal of the

(continued) excretory cell was quantified by dividing the region between the posterior bulb of the pharynx to the tip of the tail into seven segments. Percentage of canal arms terminating in each segment is indicated. Segment scoring 50% or higher was highlighted in dark blue, segment scoring 15 – 49% was highlighted light blue for easier orientation. All strains contained the *mamEx11* transgene to visualize the excretory cell. Statistical significance of differences between the strains was analysed using Fisher's exact test for 2x3 table. For the test, data from segments 0 – 4 were pooled into one category ("shorter"), data from segments 5 and 6 were used as the two other categories ("normal" and "longer", respectively). Comparison was made either to the control strain or to the more severe single mutant in the case of double mutant strains. Bonferroni correction for multiple testing was applied. C) Anterior canals of the excretory cell are shortened in *sel-5 vps-29* double mutants. Excretory cell was visualized by P*pgp-12::gfp* expression from a *mamEx29* transgene. Scale bar represents 100 µm. D) Posterior canals on the right side of the animals are more severely affected compared to their left counterparts. The length of the posterior canal on each side of the animal was measured and normalized to the length of the whole body of the animal. Paired t-test was used to assess the significance of the difference between the two sides, *** p-value < 0.001, ns – not significant. E) Posterior excretory canals are shorter already at the time of hatching in *sel-5 vps-29* mutants. The dynamics of posterior canal outgrowth was assessed by measuring the canal length and normalizing it to the total body length at hatching and at three time points during early larval development. Results are presented as mean + s.d. of at least 30 canals for each condition. Unpaired two-tailed Student's t-test was performed to assess the difference between the samples, * p-value < 0.05, ** p-value < 0.01. F) Loss of either *vps-35*, *vps-26* or *snx-3* retromer component expression induces posterior canal shortening in *sel-5* mutants. Canal outgrowth was scored as in 4B. G) Both cell-autonomous and non-autonomous expression of *sel-5* rescues excretory canal shortening in *sel-5 vps-29* mutants. SEL-5 was expressed from an extrachromosomal array under the control of *pgp-12*, *hlh-1* or *col-10* promoters. Canal outgrowth was scored as in 4B and comparison was made between animals carrying the array and their siblings which have lost the transgenic array. All strains contained also the *mamEx29* extrachromosomal array to visualize the excretory canal. H) T160 phosphorylation of DPY-23 is not required for posterior excretory canal outgrowth. Canal outgrowth was scored as in 4B in strains containing *dpy-23(mew25)* allele carrying T160A substitution. Comparison was made between the double mutants and either *sel-5* or *vps-29* single mutant. For F) – H) † – differences not significant, ‡ – same data as in B).

A

B

	0	1	2	3	4	5	6	N	p-value	versus
ctrl	0	0	0	0	1	99	0	248		
egl-20(n585)	0	0	0	0	1	93	6	169	0.0007	ctrl
cwn-1(ok546)	0	0	0	0	0	98	2	230	0.1328†	ctrl
cwn-2(ok895)	0	1	0	0	6	91	2	176	0.0008	ctrl
lin-44(n1792)	0	0	0	0	0	6	94	194	<0.0001	ctrl
mig-1(e1787)	0	0	0	0	0	100	0	180	0.5115†	ctrl
lin-17(n671)	0	0	0	0	0	14	86	175	<0.0001	ctrl
cfz-2(ok1201)	0	0	0	1	12	85	2	177	<0.0001	ctrl
mig-14(mu71)	0	0	0	0	3	14	83	182	<0.0001	ctrl
pry-1(mu38)	0	0	0	0	3	95	2	187	0.0939†	ctrl
dsh-1(ok1445)	0	0	0	0	0	84	16	232	<0.0001	ctrl
mig-5(cp385)‡	0	0	0	0	3	65	32	182	<0.0001	ctrl
lin-44; egl-20	0	0	0	0	0	10	90	180	0.1262†	*lin-44*
lin-44; cwn-1	0	0	0	0	2	43	55	204	<0.0001	*lin-44*
lin-44; cwn-2	0	0	0	1	2	24	73	181	<0.0001	*lin-44*
cwn-1; egl-20	0	0	0	1	1	96	2	180	0.2201†	*egl-20*
cwn-1; cwn-2	0	1	1	2	4	91	1	179	0.4533†	*cwn-2*
mig-1; egl-20	0	0	0	0	0	91	9	180	0.1998†	*egl-20*
mig-1; cfz-2	0	0	0	0	3	97	0	178	<0.0001	*cfz-2*
lin-17; cfz-2	0	1	1	1	8	61	28	180	<0.0001	*lin-17*
lin-17; sel-5(ok149)	0	0	0	0	0	35	65	180	<0.0001	*lin-17*
lin-44; sel-5(ok149)	0	0	0	0	7	43	50	128	<0.0001	*lin-44*

C

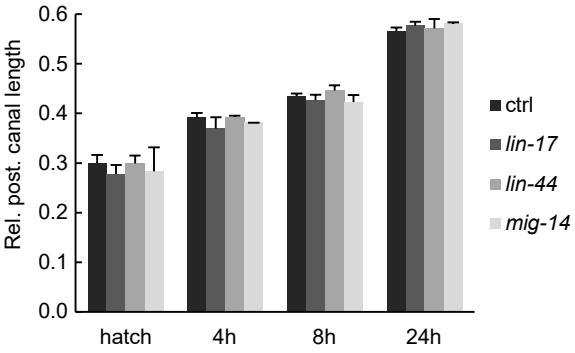

Figure 5. Wnt pathway components LIN-44/Wnt and LIN-17/Frizzled determine the stopping point for excretory canal outgrowth. A) Posterior canals of the excretory cell overgrow into the tip of the tail in *lin-17* mutants. Excretory cell was visualized by P*pgp-12::gfp* expression from the *sIs10089* transgene. Boxed areas are magnified in the bottom row, scale bare represents 200 µm. B) Quantification of posterior canal outgrowth in Wnt pathway mutants. Canal outgrowth was scored as in Fig. 4B and comparison was made either to the control strain (*sIs10089* only) or to the more severe single mutant in the case of double mutant strains. All strains contained the *sIs10089* transgene to visualize excretory canals except for *lin-17; sel-5* and *lin-44; sel-5* which contained *mamEx11*, and *mig-5*, which contained *mamEx29*. † – differences not significant. ‡ Full genotype was *mig-5(cp385[mNG-GLO^AID::mig-5]); mamEx29; mamEx34[eft-3p::TIR::mRuby; myo2p::tdTomato]* and animals were grown on NGM plates with 1 mM auxin from L1 till L4/young adult stage. Only animals containing the *mamEx34* array were used for analysis. C) Posterior excretory canals display normal length during early larval development. The dynamics of posterior canal outgrowth in *lin-44*, *lin-17* and *mig-14* mutants was assessed by measuring the canal length and normalizing it to the total body length at hatching and at three time points during early larval development. Results are presented as mean + s.d. of at least 30 measured canals. Comparison between samples assessed by unpaired two-tailed Student's t-test did not reveal any significant differences.

A

	0	1	2	3	4	5	6	N	p-value	versus
mig-10	8	84	8	0	0	0	0	173		
sel-5 mig-10	11	70	19	0	0	0	0	432	0.0007	*mig-10*
mig-10 vps-29	11	78	11	0	0	0	0	349	0.3517†	*mig-10*
mig-10; L4440 RNAi	6	58	36	0	0	0	0	67		
mig-10; vps-29 RNAi	5	64	31	0	0	0	0	97	0.7423†	*mig-10; L4440 RNAi*
mig-10; vps-35 RNAi	11	65	24	0	0	0	0	75	0.2315†	*mig-10; L4440 RNAi*
sel-5 mig-10; L4440 RNAi	9	69	22	0	0	0	0	268		
sel-5 mig-10; vps-29 RNAi	23	71	6	0	0	0	0	331	<0.0001	*sel-5 mig-10; L4440 RNAi*
sel-5 mig-10; vps-35 RNAi	76	22	2	0	0	0	0	92	<0.0001	*sel-5 mig-10; L4440 RNAi*

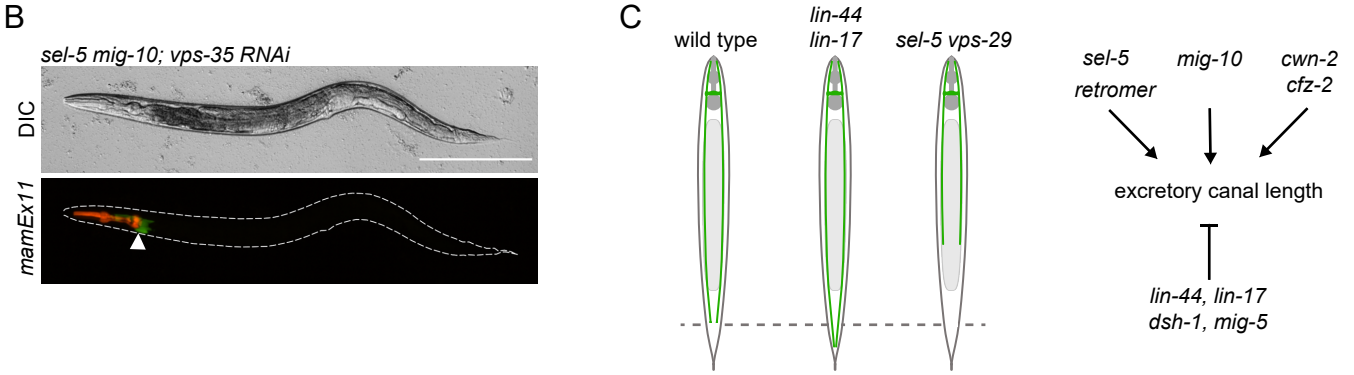

Figure 6. SEL-5 and retromer genetically interact with MIG-10/Lamellipodin in excretory cell outgrowth. A) The length of the excretory cell posterior canals was assessed in *mig-10* mutants and after simultaneous loss of *mig-10* and *sel-5* or the retromer or both. Canal shortening was determined as in Fig. 4B, statistical comparison was made to the appropriate control condition. For the Fisher's exact test data from segments 0, 1 and 2 were used as the three tested categories. All strains contained the *mamEx11* transgene. B) Complete lack of posterior canal outgrowth in *sel-5 mig-10* animals treated with *vps-35* RNAi. Co-injection marker P*myo-2::tdTomato* expression labels the pharynx of the animal, white arrowhead points to the excretory cell body. C) Model summarizing the effect of various mutants on the outgrowth of the excretory cell posterior canals. On the left, the three possible outcomes of canal outgrowth are outlined. In wild type animals posterior canals reach to the level of rectum (dashed line). In *lin-44* or *lin-17* mutants, a putative stop signal is missing and the canals grow past the rectum into the tip of the tail. On the other hand, simultaneous loss of *sel-5* and the retromer complex components prevents the canals to reach the wild type position. Several inputs are integrated to define the proper length of posterior excretory canals; those discussed in this work are summarized on the right.